

EFFICIENCY MEASUREMENTS ON THIN FILM SOLAR CELLS WITH DIFFERENT TEXTURIZED SURFACES AND TCO THICKNESSES

Bachelors Thesis

By:
Yalda Mohammadian, 3157768
1-8-2012

Supervised By:
M.M. de Jong Msc.
Dr. J.K. Rath

At:
Utrecht University,
Department of Physics and Astronomy,
Debye Institute for Nanomaterials Science
Physics of Devices

CONTENTS

1	Introduction.....	3
1.1	Aim of Research.....	5
1.2	Proposed Method of Research.....	6
1.3	In This Thesis.....	6
2	Theory of Solar Cells	7
2.1	Semiconductors.....	7
2.2	Doping.....	8
2.3	P-N Junction	9
2.4	Structure of Solar Cells.....	9
2.5	P-I-N Junction	10
2.6	Types of Solar Cells	10
2.7	Efficiency.....	12
3	Experimental Method.....	13
4	Results.....	15
4.1	Results of Optical Measurements With The Perkin-Elmer.....	16
4.1.1	Substrate I.....	16
4.1.2	Substrate II.....	17
4.1.3	Substrate III.....	18
4.2	Results of Solar Simulator Measurements	19
4.2.1	Substrate I-750.....	19
4.2.2	Substrate I-1000.....	19
4.2.3	Substrate I-2000.....	19
4.2.4	Substrate II-750.....	20
4.2.5	Substrate II-1000	20
4.2.6	Substrate II-2000	20
4.2.7	Substrate III-750	20
4.2.8	Substrate III-1000.....	21
4.2.9	Substrate III-2000.....	21
5	Conclusion.....	21

5.1	Optical Measurements Conclusion	21
5.2	Solar Simulator Measurements Conclusion.....	21
6	Discussion.....	23
6.1	Further Research	23
7	Acknowledgements	24
8	Bibliography	25
9	Tables and Figures.....	26
9.1	Solar Simulator Tables and Figures	26
9.1.1	Graph & Table of Substrate I-750.....	26
9.1.2	Graph & Table of Substrate I-1000.....	27
9.1.3	Graph & Table of Substrate I-2000.....	28
9.1.4	Graph & Table of Substrate II-750	29
9.1.5	Graph & Table of Substrate II-1000.....	30
9.1.6	Graph & Table of Substrate II-2000.....	31
9.1.7	Graph & Table of Substrate III-750.....	32
9.1.8	Graph & Table of Substrate III-1000.....	33
9.1.9	Graph & Table of Substrate III-2000.....	34

1 INTRODUCTION

To ensure a clean and sustainable environment for future generations, research and investment in renewable energies is important. Moreover oil reserves are depleting, so we have no choice but to look for other (more sustainable) ways to supply in our energy needs in the future.

One possible sustainable energy source is solar energy. The intensity of the solar energy reaching Earth's atmosphere is around 1370 W/m^2 [8]. If we multiply this with the cross section of the earth, and divide it with the surface area of the earth, we get the average solar energy per square meter.

$$\frac{1370 \times \pi R_{earth}^2}{4\pi R_{earth}^2} = \frac{1370}{4} \approx 342 \text{ W/m}^2$$

Not all of this energy reaches the surface of the earth, for some of it is reflected by the clouds and some of it is absorbed by the atmosphere as you can see in the picture below (Figure 1.1). On average, around 200 W/m^2 gets through and hits the surface of the earth.

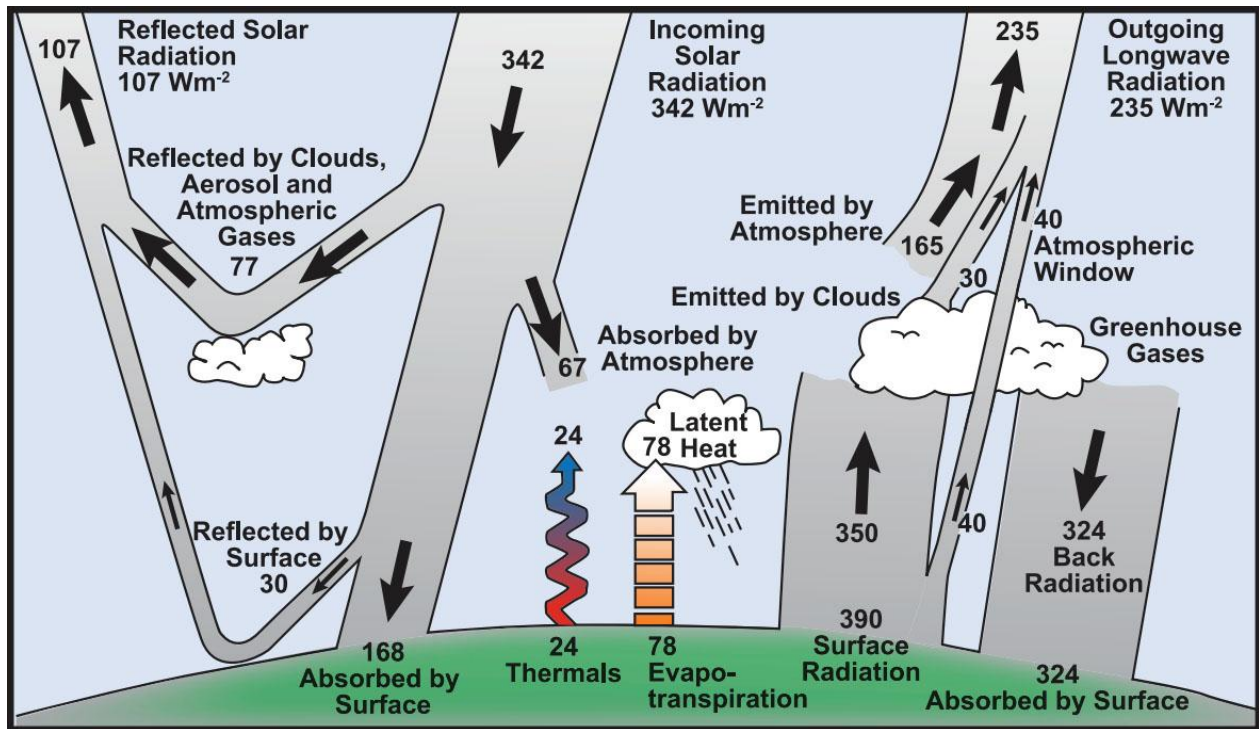


Figure 1.1 - The left side of this picture shows a graphical representation of the solar energy balance. As you can see, around 200 W/m^2 of the solar energy reaches the earth's surface (this is the amount absorbed plus reflected by the earth) [8].

Over the entire earth's surface (with $R_{earth} = 6371 \text{ km}$), this equals to a total average annual energy of:

$$200 \times \pi R_{earth}^2 \times 3600 \times 24 \times 365.25 = 8.05 \times 10^{23} \text{ Joule/year} \quad (1.1)$$

In 2008, the global energy consumption was estimated to be $505 \times 10^{15} \text{ Btu}$ [9], which converts to $5.33 \times 10^{20} \text{ Joule}$. Assuming that we would be able to convert 10% of the Sun's energy into useful energy with the use of solar panels, only **0.66%** of the earth's surface area would be needed to be covered with solar panels to satisfy the worlds energy needs in a sustainable manner. And if you

succeed in increasing the efficiency of solar cells, you can decrease this number further. This is why solar energy is so interesting, for it can, in theory, meet all our energy needs. For this reason, a lot of effort has been put over the years into improving the efficiency and cost of solar cells.

In 2010, 16.7% of the global energy consumption came from renewable energy sources [6]. Modern renewable energies accounted for 8.2% of this number, while 8.5% came from biofuels. Fossil fuels accounted for 80.6% of the global energy consumption and nuclear energy for the remaining 2.7%. See Figure 1.2 for a graphical representation.

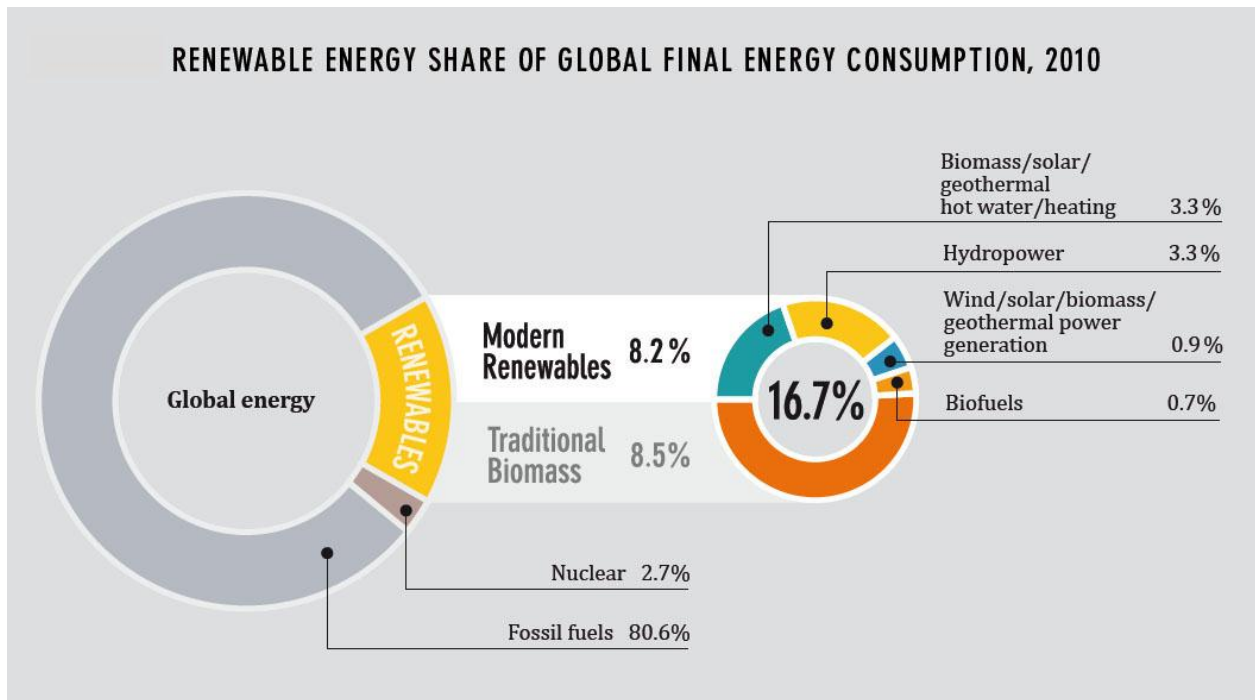


Figure 1.2 - Renewable energy share of global final energy consumption [6].

Although the total solar PV capacity at the moment is still less than 1% of the global energy consumption, it is the fastest growing renewable technology (see Figure 1.3). In the last decade, a lot has been done to increase the efficiency, and above all, to decrease the cost of solar panels. As a result, in the period of end-2006 through 2011, solar PV has increased its operating capacity with an average of 58% each year. In the year 2011 alone, the global solar PV operating capacity increased by 74% to 70 GW.

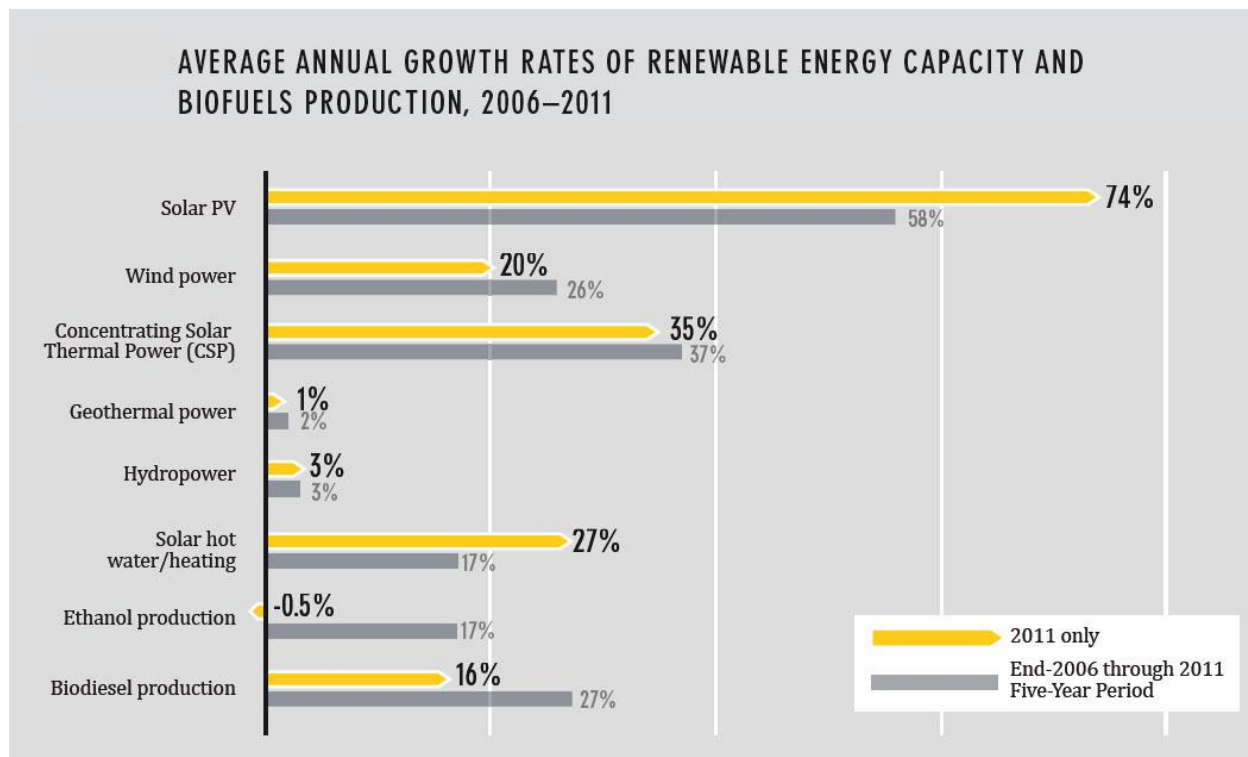


Figure 1.3 - Average annual growth rates of renewable energy capacity [6].

1.1 AIM OF RESEARCH

In our effort to increase the efficiency of (in our case thin film) solar cells, a method called light trapping can be used to “trap” the incoming light in the active layer as to increase the distance of which the light travels through the active layer. For amorphous silicon (a-Si) thin film solar cells on plastic substrates, light trapping using micro-pyramidal (10 μm base) and submicron-pyramidal (400 nm base) substrate structuring has been shown to increase efficiency compared to cells with a flat surface [1]. Because of these pyramidal structures, the incoming light rays hit the surface at an angle and are refracted, as a result the light rays travel through the active layer at an angle. This increases the traveling distance. Moreover the pyramidal structures help trap the light inside the active layer if they are reflected by the second (back) layer. A negative side effect of these pyramidal structures though is, that they sometimes can lead to deterioration of the electrical properties, resulting in a lower V_{oc} , a lower Fill Factor and hence a lower efficiency [5].

In this study we would like to find out if we can find ways to have both excellent light trapping and electrical properties. We will be using three different types of polycarbonate substrates, one with a pyramidal structure with a base of 10 μm , one with a pyramidal structure with a base of 400 nm , and one with an anti-pyramidal structure with a base of 400 nm . On those we will deposit a-Si solar cells in a p-i-n configuration. Because our structured substrates are made from polycarbonate, we are limited in our substrate temperature to around 130 °C. And since temperature plays a very important role in silicon depositions, our material has more defects and a higher structural disorder, which is directly reflected in the electrical cell properties. On these substrates we want to grow, as a front contact, a transparent conductive oxide (TCO), for which we will be using aluminum doped zinc-oxide (ZnO:Al).

A TCO thickness of 1000 *nm* or higher is common, but increasing thicknesses on a texturized surface will result in the increasing smoothing out of the substrate surface. A difference in the thickness of our TCO (ZnO:Al) consequently will result in a difference in light trapping effectiveness and the electrical properties of the cell. We are interested in knowing what thickness gives us an optimum performance for the combined light trapping and electrical properties of the cell, and consequently resulting in higher efficiencies.

1.2 PROPOSED METHOD OF RESEARCH

To find out what thickness of zinc-oxide results in the highest efficiency, we make a series of substrates with different thicknesses of zinc-oxide deposited on them. This can be done using the sputter deposition system called SALSA.

In advance to depositing a-Si solar cells on these substrates, we do transmission and reflection measurements of the substrates in order to see what fraction of the light is reflected, transmitted and diffusively transmitted by our TCO-substrate combination. The Perkin-Elmer is used for these measurements.

Moreover, we do some kind of surface topology and roughness measurements to see to what extent the surface has flattened after deposition of our TCO. For our submicron-pyramidal textured substrates we can use the Atomic Force Microscopy (AFM), and for the micro-pyramidal textured substrates the DekTak to do surface topology measurements.

Then we are ready to deposit a-Si solar cells on our substrates using the ASTER deposition system, and measure their optical and electrical characteristics. The Solar Simulator (SS) is used for current density voltage (J-V) measurements, from which we can derive the maximum power peak, P_{max} , which is the maximum power that can be obtained from the solar cell with a certain J and V (giving us the conversion efficiency), and we can derive the Fill Factor of the cell which gives us a feel for the efficiency of that cell. These measurements is done under Standard Test Conditions (STC) of ambient temperature of 25 °C, AM1.5 spectrum.

1.3 IN THIS THESIS...

In this thesis we will shortly discuss the theory behind solar cells. To do that we will briefly go through what semiconductors are, what doping is and why it is necessary in solar cells and what a p-n junction is, also explaining our used p-i-n configuration. Furthermore we will give a rough outline of how a solar cell is made and discuss two of the most commonly used types of solar cells. Finally we will explain what contributes to solar cell efficiency, and how this efficiency can be expressed and/or measured.

Then we will explain the methods of my research and discuss any difficulties that we came across. The results will be given next. We will interpret them and give a conclusion based on these results. Finally we will talk over the possibilities for improvements or for further research.

2 THEORY OF SOLAR CELLS

2.1 SEMICONDUCTORS

Most solar cells are made out of materials called semiconductors. These are a special kind of material whose conductivity is larger than that of insulators but smaller than that of conductors. Common types of semiconductors are crystalline solids which are organized in a crystal lattice. This means that they are structured in an organized manner. Each atom in this crystal lattice has some of its electrons in its outermost shell, the valence band. These electrons are accordingly called valence electrons. In the case of crystalline silicon, there are a total of four valence electrons.

In order to free an electron from its lattice, from the valence band into the conduction band, you need a minimum amount of energy known as the band gap energy E_g . When a photon with sufficient energy, $E_{ph} = h \cdot \nu > E_g$ (h being Planck's constant and ν the photon's frequency), hits the semiconductor, it liberates an electron from the valence band into the conduction band, increasing conductivity and leaving a "hole" behind. This phenomenon is called the photovoltaic effect.

When an electron is released from its valence band due to the photovoltaic effect, it leaves behind a "hole" in the crystal lattice. An electron from a nearby atom's valence band can now fill this hole, causing a new hole to be created in the adjoining atom. In this manner a hole can move from atom to atom and thus move freely through the semiconductor, just like an electron in the conduction band can. Holes therefore also increase conductivity. When an electron in the conduction band collides with a hole, they cancel each other out by recombination.

High temperatures results in an increase in free electrons and the electrical conductivity. For a given temperature, higher band gap energies means less electrons being liberated. On the other hand, higher temperatures mean more electrons being boosted into the conduction band and as a result increasing the electrical conductivity.

During the process of photovoltaic effect, photons with energies higher than E_g , transfer this extra energy into the kinetic energy of the released electron. Due to internal friction though, this kinetic energy is eventually lost as heat. On the other hand, photons with energies less than E_g , do not have enough energy to lift an electron from the valence band into the conduction band and therefore these photons are not absorbed. This means that some energy will always be lost due to these two processes of spectral mismatch. In Figure 2.1 you can see a sketch of the fraction of the total energy used for generating electron/hole pairs.

When an electron is lifted into the conduction band by a photon with high enough energy, it will immediately want to go back to a state with the lowest amount of energy. This means that the electron will want to recombine with the hole left behind within a short amount of time if nothing is done to keep them separated. One way to do this is by inducing an electrical field within the semiconductor, causing the electron and hole to move in the opposite direction. Such a strong internal electric field within the semiconductor is created without the use of an external voltage source by using a p-n junction. This is a junction between a p-type and an n-type semiconductor. These p-type and n-type semiconductors are created by a method called doping. This mechanism of

separating electron-hole pairs forms the basis for solar cells. That is why we will explain shortly what doping is, how such a junction is created with the use of these doped semiconductors, and how a p-n junction works.

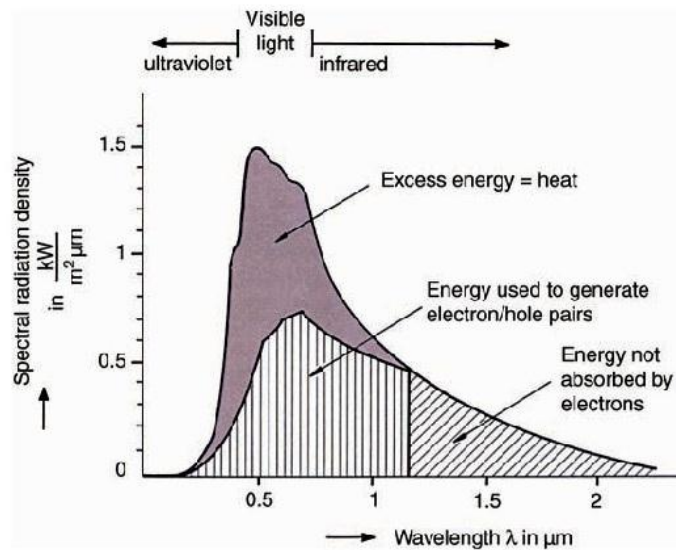


Figure 2.1 – Fraction of energy usefully used to generate electron/hole pairs [3].

2.2 DOPING

To increase the conductivity of a semiconductor, suitable external atoms are added to the semiconductor in a process called doping. If, for example, a silicon atom in the crystal lattice is replaced by a phosphorous atom, one of the five covalent electrons of the phosphorous atom cannot form a bond with adjacent atoms. This electron can then, with a minimum amount of energy, liberate itself from the phosphorous atom, leaving a positively charged phosphorous atom behind. The phosphorous atom in this case is referred to as the donor, because it “donates” an electron to the conduction band. The electron is called the donor electron. The energy to free the donor electron can be obtained from the vibration of the donor atom at high enough temperatures. Because of the release of negative charge carriers in a phosphorous doped semiconductor, this type of semiconductor is called n-conductive or n-type.

The opposite of this can be achieved by replacing a silicon atom in the crystal lattice by a boron atom. The boron atom has only three covalent electrons, which means that an electron is missing in the lattice. This is the same thing as a positive charge carrier or a hole. An electron from an adjoining atom can subsequently fill this hole if only a small amount of energy is provided. Again this energy can be obtained from temperature induced vibrations of the atoms. The boron atom in this case is also referred to as the acceptor because it “accepts” an electron from a nearby atom. The electron, by filling the hole, creates a negatively charged boron atom and allows another hole to be created at the place of the adjoining atom. As described before, holes can in this way move freely through the semiconductor and can be seen as positive charge carriers. For this reason boron doped semiconductors are called p-conductive or p-type.

After doping, n-type semiconductors now have permanent positive ions in the crystal lattice, because the donor atom has given away one of its electrons. The opposite goes for p-type

semiconductors, which have permanent negative ions in the crystal lattice, because the acceptor has accepted one electron.

For crystalline silicon cells, solar grade pure silicon is needed. To produce silicon of such extreme purity, several processes are needed which are carried out at very high temperatures (1200 °C). Dopings are made in high temperature diffusion processes. This makes the doping of crystalline silicon cells extremely energy and therefore expensive process. For thin film solar cells such extreme purities aren't needed, in addition to low temperature processing, which is why thin film solar cells are less expensive to make.

2.3 P-N JUNCTION

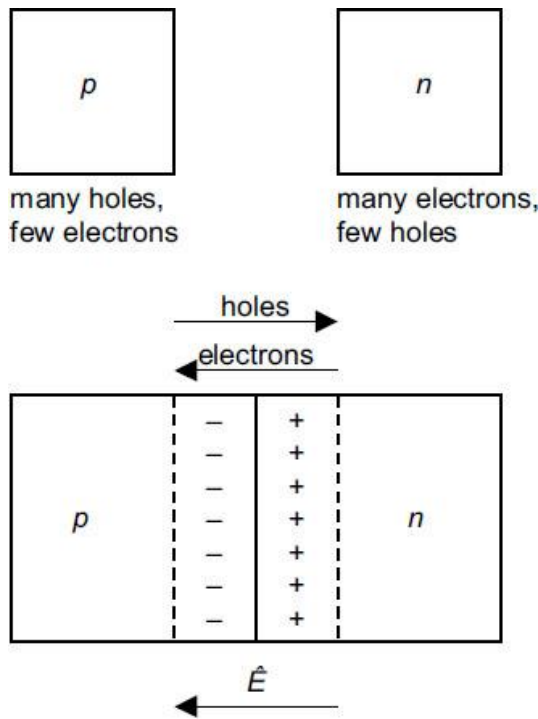


Figure 2.1 - Electric field created inside semiconductor with use of p-n junction. The section between the dashed lines is the space charge region [10].

When putting an n-type semiconductor against a p-type semiconductor, a so called p-n junction is created. The free moving electrons in the n-zone can now move freely into the p-zone and recombine with the holes there and vice versa. Because of the positive donor atoms left behind in the n-zone (remember that they cannot move since they are stuck in the crystal lattice) and the negative acceptor ions in the p-zone, a difference of charge is created near the junction which produces a strong internal electric field (see Figure 2.2) with a potential difference, called diffusion potential, V_d . This region is called the space charge region.

The electric field that as a consequence is created can now be used to separate electron-hole pairs created by the internal photoelectric effect in the space charge region. As more donor electrons and holes recombine, the field gets stronger until eventually it gets strong enough to prevent donor electrons and holes to cross the space charge region and recombine. The field then stops growing.

The junction becomes a diode if metal contacts are integrated on each side. A solar cell is in fact a

semiconductor diode. P-n junctions are usually used for crystalline silicon solar cells. For thin film solar cells, however, p-i-n junctions are more common. The principles of these types of junctions will be explained in Chapter 2.5.

2.4 STRUCTURE OF SOLAR CELLS

A solar cell is usually made using a diode, which, in our case, consists of a p-i-n junction with metal contacts on the front and back side. One side will be facing the light, so to allow for as much light as possible to reach the space charge region, the contacts on this front end must shade only a minute surface area, or it has to be transparent. An anti-reflection coating is also applied as to minimize the reflection of light at the surface. Furthermore we want to make sure that the electron-hole pairs

created by the internal photoelectric effect are created in the space charge region so they can be separated from each other before recombining. This is why the doped semiconductor zone (p-zone or n-zone) facing the light must be very thin.

When electron-hole pairs are created in a p-n junction, these are separated by the electric field present in the space charge region. Released electrons accumulate in the n-zone and the holes in the p-zone. This causes another electric field to be created in the opposite way of the electric field in the space charge region, thus causing the electron field in the space charge region to be reduced until it is not strong enough to separate electron-hole pairs. This is when the solar cell reaches its open-circuit voltage V_{oc} . The open circuit voltage is always less than V_d .

The short circuit current density, J_{sc} , is obtained by connecting the front and back contacts, consequently short circuiting the diode. The separated electrons and holes can now flow through the wire out of their respective zones. The current density this creates is called the short circuit current density J_{sc} . It is proportional to the amount of electron-hole pairs being separated each second in the space charge region and therefore proportional to the irradiance G if there is no recombination.

2.5 P-I-N JUNCTION

As will be explained below (section 2.6) there are many different types of solar cells. Two of the most common are crystalline silicon (c-Si) and amorphous silicon (a-Si) solar cells. The structure of a-Si differs from that of c-Si in that it has many “defects” in its structure which give rise to so called “dangling bonds” (the concept will be explained below, a graphical representation is given in Figure 2.3). In doped a-Si, the density of these dangling bonds are two or three orders of magnitude higher than in undoped (called intrinsic) a-Si [12]. These dangling bonds promote recombination. Hence, to minimize the recombination inside a solar cell, an intrinsic a-Si layer (with less dangling bonds) is sandwiched between the n-type and p-type layers, thereby creating a p-i-n junction. Due to the n-type and p-type layers, as with the p-n junction, an internal electric field will arise across the intrinsic layer which will help separate the electron-hole pairs.

2.6 TYPES OF SOLAR CELLS

Semiconductors can be categorized into two groups, namely directly absorbent and indirectly absorbent semiconductors. With directly absorbent semiconductors, material of around only $1\mu\text{m}$ is needed to fully absorb all photons with high enough energy, whereas with indirect absorbent semiconductors you need at least a thickness of $100\mu\text{m}$ in order to absorb all photons ([3], page 80). The thickness needed for semiconductors can be reduced by using “light trapping” techniques which increase the optical path of light through the semiconductor. This is achieved by making use of a texturized surface which allows incoming light to be refracted at the surface and, thus, going through the semiconductor at an angle, which in turn increases the optical path. Moreover, a reflective back side is used to reflect any light not absorbed by the semiconductor, allowing for another pass through the semiconductor.

The most commonly used type of solar cells is the crystalline silicon (c-Si) solar cell. Crystalline silicon is an indirect absorbent semiconductor, this means that you need a thick slice (wafer) to assure that all the photons with high enough energy are absorbed. To produce these types of solar

cells however, you need to have extremely pure crystalline silicon, the production of which, because of the very high temperatures needed, is very energy intensive. Also a lot of material is lost during the sawing of the silicon ingots into wafers.

The energy cost of directly absorbent semiconductors is a lot less in comparison with the energy cost of indirectly absorbent semiconductors as less material is needed. A thin film of $0.5 \mu\text{m}$ to $5 \mu\text{m}$ of a directly absorbent semiconductor is sufficient to fully absorb all photons with high enough energies. These types of solar cells are therefore called thin film solar cells. One type of thin film solar cell is the amorphous silicon (a-Si) solar cell. Because of the reduced thickness of these thin film solar cells, the silicon can be vapor deposited on a substrate. This means that to produce these solar cells, temperatures of only around $100 - 200 \text{ }^\circ\text{C}$ are needed instead of the $1200 \text{ }^\circ\text{C}$ needed for crystalline silicon.

The structure of amorphous silicon differs from that of crystalline silicon in that its crystal lattice is organized less regularly, i.e., only short range order, it has a more random structure. Because of this random structure, not every silicon atom is connected with another, which means that there are a lot of electrons available from dangling bonds (see Figure 2.3). The imperfections in the crystal lattice therefore promote recombination as the electrons can recombine with holes created by the photovoltaic effect. To get rid of these dangling bonds, hydrogen atoms can be added (Si:H) to bond with them. In practice though, you cannot get rid of all the dangling bonds this way. Also, as the material “sets” and is exposed to light for the first time, more bonds are broken during the first few weeks, creating more dangling bonds in the lattice. These imperfections, together with the higher band gap energy of the amorphous silicon cells, are the main reasons for reduced efficiencies seen in a-Si cells compared to crystalline solar cells. But as a-Si solar cells are easier and cheaper to produce, they are still very interesting.

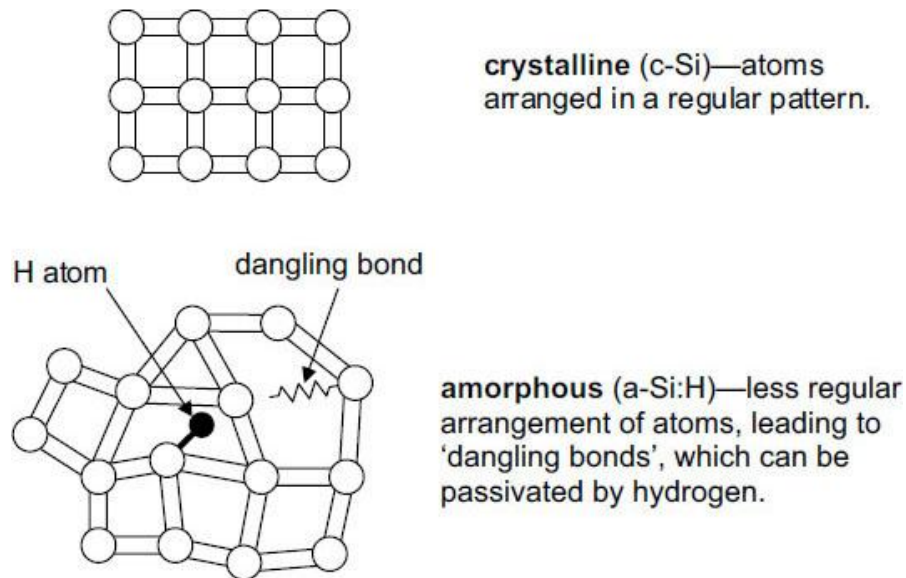


Figure 2.2 - Difference between Crystalline Silicon and Amorphous Silicon [10].

2.7 EFFICIENCY

The conversion efficiency of a solar cell can be measured by dividing its maximum power (in watts) with the product of the irradiance G (W/m^2) with the surface area A_{cell} (m^2). This gives the percentage of solar energy being converted into electrical energy.

$$\eta_{conv} = \frac{P_{max}}{G \cdot A_{cell}} \quad (2.1)$$

This efficiency is determined by several factors.

The factors that affect the conversion efficiency are for example thermodynamic efficiency, (external) quantum efficiency, conduction efficiency etc. Furthermore the values of J_{sc} and V_{oc} are proportional to the cell's temperature. A different temperature results in a different value of P_{max} , consequently affecting the conversion efficiency. An example of an I-V curve is shown in Figure 2.4, also the power is given as a function of the voltage V .

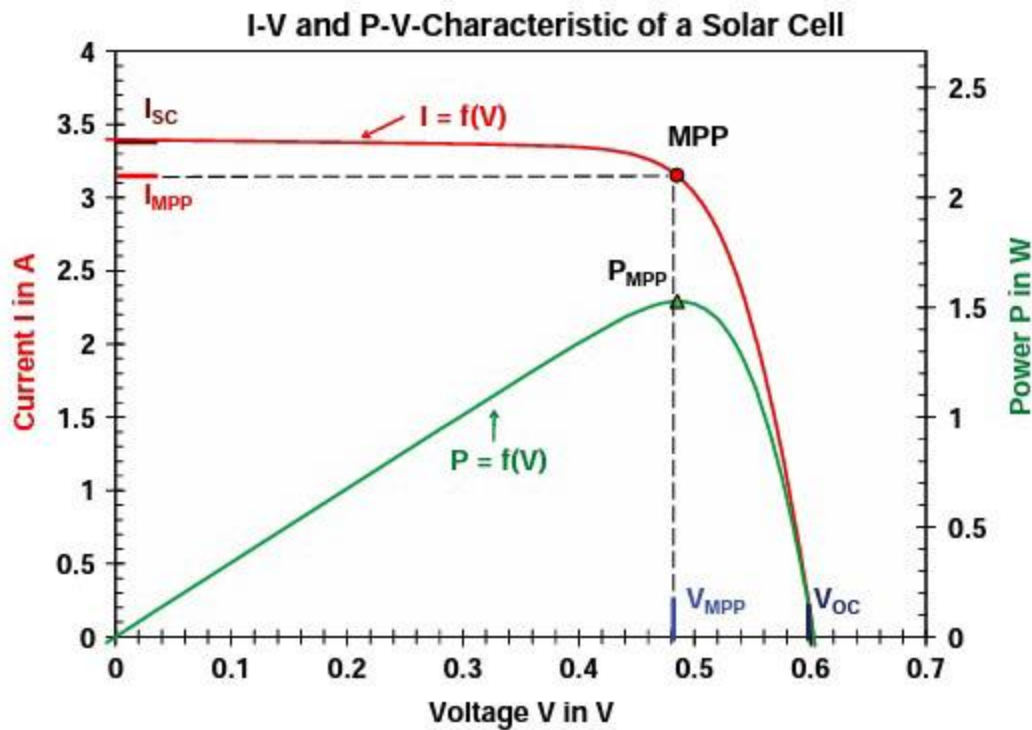


Figure 2.3 – An example of an I-V and a P-V curve showing the current I and the power P as a function of V . Also indicated in the figure, the maximum power point P_{max} , the short circuit current I_{sc} and the open circuit voltage V_{oc} .

The thermodynamic efficiency is the amount of energy from the photons that can be converted to a useful output (in this case a current). As explained before, photons with insufficient energy cannot free a valence electron from its bond, so the energy of these photons cannot be used. On the other hand, photons with energies higher than the band gap energy convert this extra energy into the kinetic energy of the released electron. The electron however loses it again to heat because of friction within the material. So again some energy is lost here. The optimum semiconductor band gap energy that maximizes the thermodynamic efficiency for sunlight on earth is 1.5 eV, as it has the

best balance between energy lost due to photons of low energy and energy lost due to photons with too high energies (see Figure 2.5).

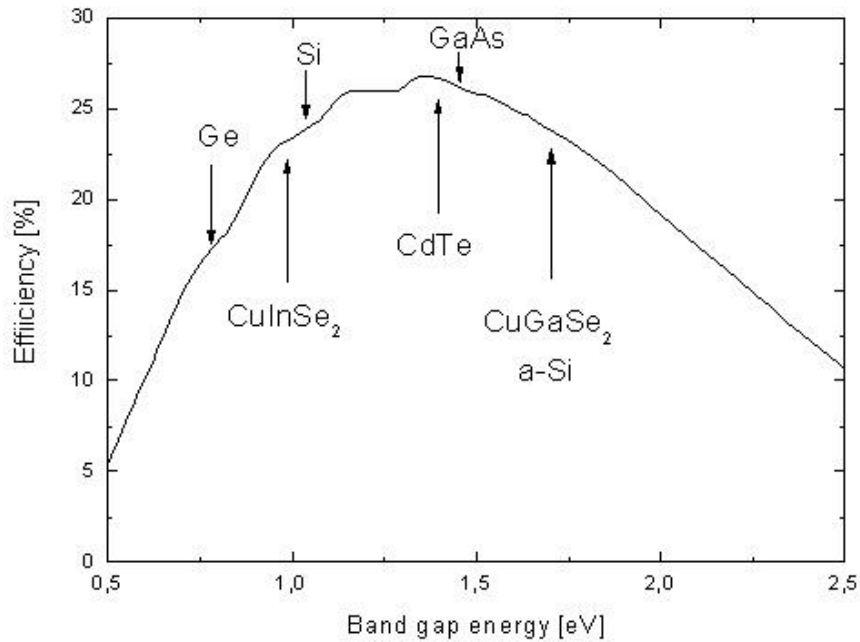


Figure 2.4 - The theoretical maximum achievable efficiency for a certain band gap value [4].

The quantum efficiency refers to the percentage of photons that create charge carriers inside the space charge region (and thus creating a current). The external quantum efficiency also accounts for losses due to reflection because it gives the amount of incident photons that are converted to electrical current. Quantum efficiency can be measured in spectral response measurement. By measuring what percentage of light with a certain wavelength passes through and are reflected, one can calculate what percentage of the photons are absorbed and thus create an electron-hole pair.

Finally the conduction efficiency refers to how well the semiconductor material conducts a current. Solar cells with low conduction efficiency have a low conductivity and large resistance. Within these cells, a large portion of the electrical energy is lost to heat.

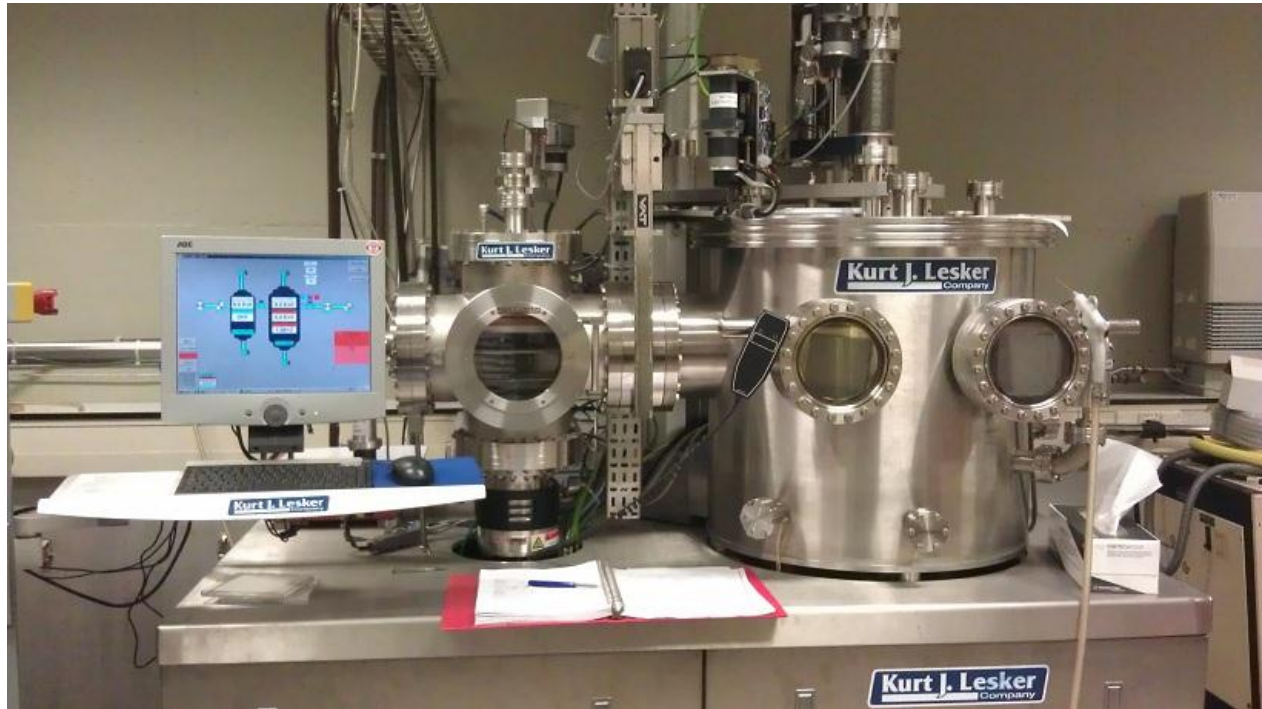
One other useful way to understand the electronic quality of a solar cell is the Fill Factor, given by:

$$FF = \frac{P_{max}}{V_{oc} \cdot J_{sc}} = \frac{\eta_{conv} \cdot G \cdot A_{cell}}{V_{oc} \cdot J_{sc}} \quad (2.2)$$

It gives a measurement of how well the square of $V_{max} \times J_{max}$ fills the square of $V_{oc} \times J_{oc}$ (see Figure 2.4).

3 EXPERIMENTAL METHOD

To find out what thickness of zinc-oxide results in the highest efficiency, we made a series of substrates with different thicknesses of aluminum doped zinc-oxide deposited on them. This was done in the RF magnetron sputter deposition system, called SALSA (see Picture 3.1).



Picture 3.1 – Our RF magnetron sputter deposition system called SALSAs.

We used three different types of substrates: Substrate I with an anti-pyramidal structures, each with a base of 400 nm , Substrate II with pyramidal structure, each with again a 400 nm base and Substrate III with pyramidal structures, each with a $10\text{ }\mu\text{m}$ base. On each type of the substrates, we deposited four different thicknesses of ZnO:Al: 750 nm , 1000 nm , 1500 nm and 2000 nm . For each substrate/thickness combination, we made one larger rectangular piece for our a-Si solar cell deposition, and a smaller square piece for measurements in the Perkin-Elmer and AFM/DekTak (see Picture 3.2). For further convenience, we will be referring to the substrates/thickness combination as I-750 for Substrate I with an ZnO:Al deposition of 750 nm , or II-1500 for Substrate II with a 1500 nm deposition etc.

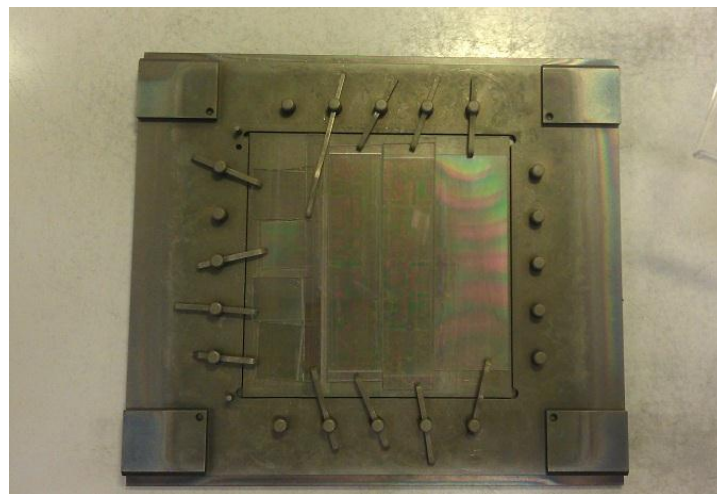


Figure 3.2 – One set of substrates ready to be used in SALSAs.

Using the smaller substrates, we did transmission and reflection measurements in order to see what fraction of the light is reflected, transmitted, or diffusively transmitted. If it is diffusively transmitted, this means that the light is refracted or scattered at the surface and will go through our active material at an angle. For these measurements, the Perkin-Elmer was used. Halfway through the measurements, however, it became apparent that the 1500 nm substrates were too small to fill the entire opening of the Perkin-Elmer, through which light was sent. For this reason another batch of small 1500 nm substrates had to be made.



Figure 3.3 - The Perkin Elmer

We also wanted to do some topology and roughness measurements of the surface of the substrates to see how the ZnO:Al layer affects the texture of the substrates. However, we had some trouble in getting the AFM to work. Possibly the material of our substrates (polycarbonate) was too soft to be able to do accurate measurements. For this reason we decided not to do any surface measurements at all and leave this as a suggestion for further research, perhaps measurements can be made using a different device.

Finally we were ready to deposit, using the ASTER system, a-Si solar cells on our larger substrates and measure the optical and electrical characteristics of these cells. Unfortunately during the process of a-Si solar cell deposition, we lost our 1500 nm substrates. With the rest of the substrates, the Solar Simulator (SS) under STC was used for current density-voltage (J-V) measurements, from which we can derive the maximum power (P_{max}) and Fill Factor. The conversion efficiency can be calculated using the formula mentioned earlier (Equation 2.1).

4 RESULTS

4.1 RESULTS OF OPTICAL MEASUREMENTS WITH THE PERKIN-ELMER

For the data resulting from the optical measurements by the Perkin-Elmer, we used the program "Origin 8.0" to plot the data into a graph. We made separate graphs for every substrate/thickness combination, showing the total reflection, total transmission and diffuse transmission. In the following section we will show the four graphs of each Substrate, and discuss any differences.

4.1.1 SUBSTRATE I

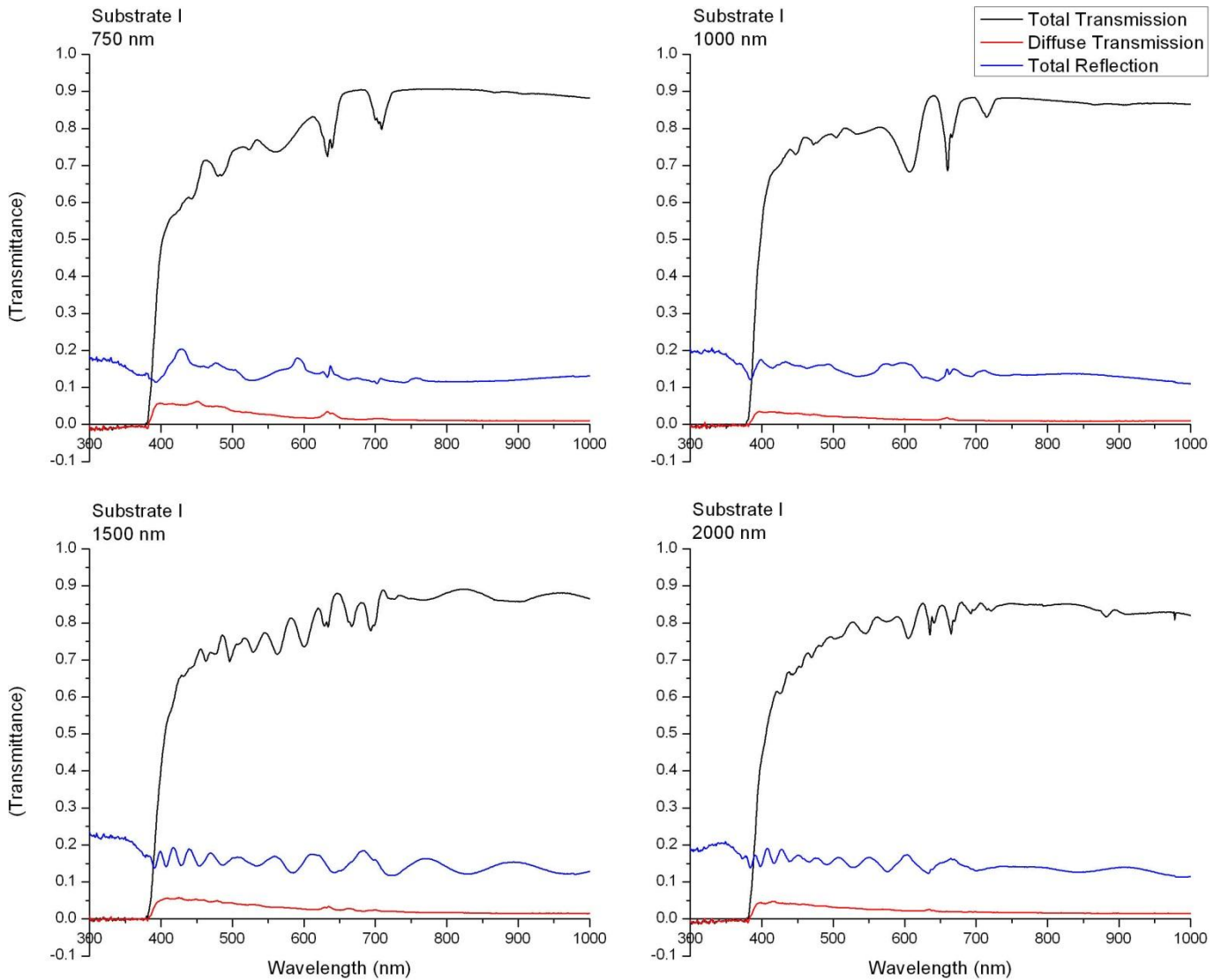


Figure 4.1 – Optical measurements results for Substrate I. For each TCO thickness of Substrate I, you can see the total and diffuse transmission and total reflection as a function of the wavelength.

In Figure 4.1 you can see the graphs of Substrate I for the four different thicknesses of ZnO:Al. The total transmission, diffuse transmission and total reflections are shown as a function of the wavelength. As one can see, there is no clear difference between the different graphs. One small

difference that can be seen is that the total transmission gets larger for wavelengths between 400 nm and 650 nm, as the TCO layer gets thicker. This is not something that one would expect, because it would be more logical for thicker TCO layers to absorb more light. One other notable thing is that one can see a slightly larger diffuse transmission with the 750 nm layered substrate than with the rest. This is in accordance with our theory that larger layers might flatten the substrate surface. This will cause less light to be scattered at the surface and transmitted through the substrate at an angle (which is what diffuse transmission is).

4.1.2 SUBSTRATE II

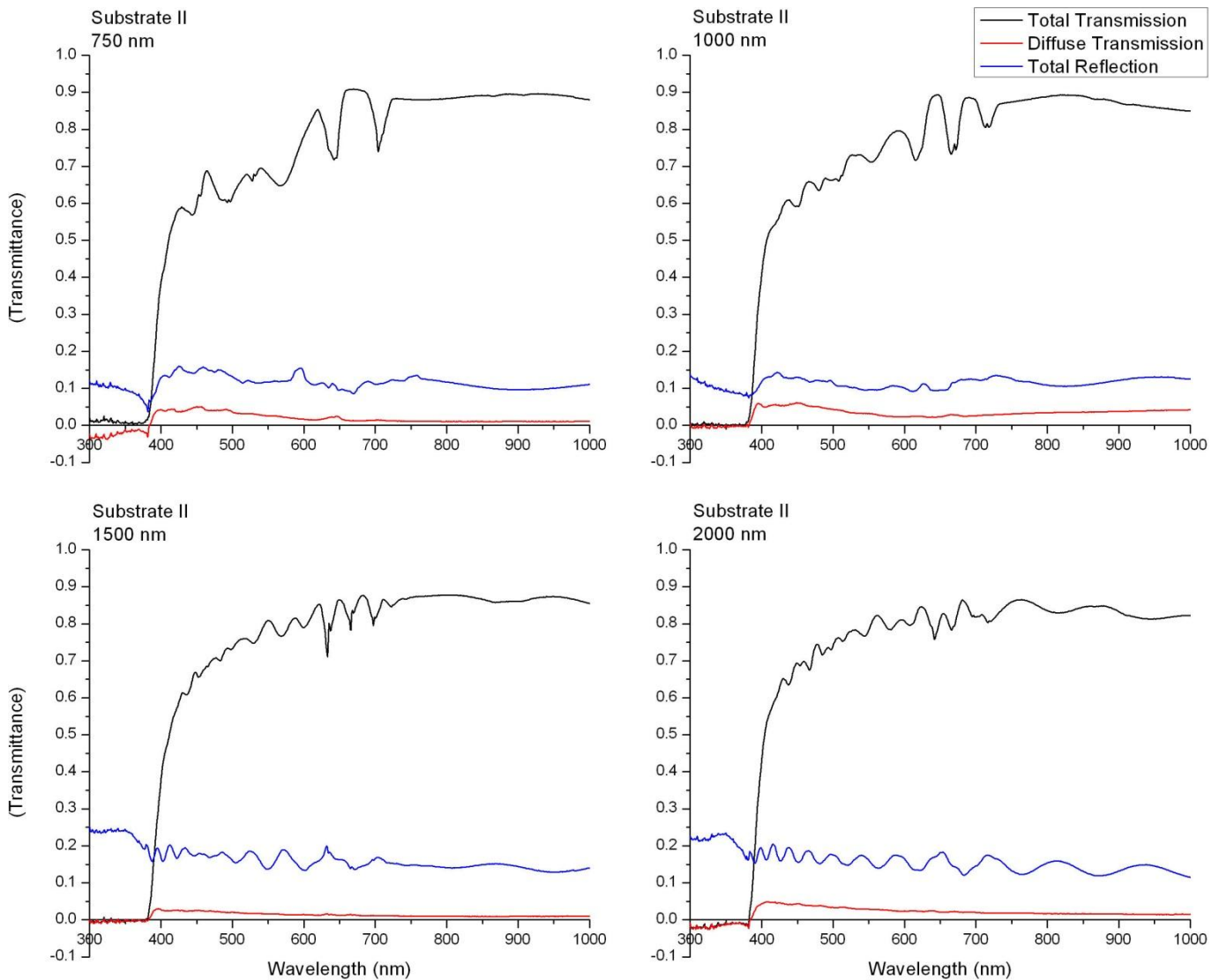


Figure 4.2 – Optical measurements results for Substrate II.

The results of measurements on Substrate II are very similar to the results of Substrate I. This is expected as they both have the same submicron-pyramidal structure (400 nm), the only difference though is that Substrate I has an anti-pyramidal structure whereas Substrate II has a pyramidal structure.

Yet again, there are no huge differences between the different TCO thicknesses. But similarly to Substrate I, one can see an increase in total transmission for wavelengths between 400 nm and 600 nm for larger TCO thickness. For Substrate II-1500, the diffuse transmission seems to be less than the other three. The diffuse transmission is probably highest for the 750 nm Substrate. Although this does not show in the graph, this is probably due to poor calibration, since one can see a negative transmittance for diffuse transmission for wavelengths under 400 nm.

4.1.3 SUBSTRATE III

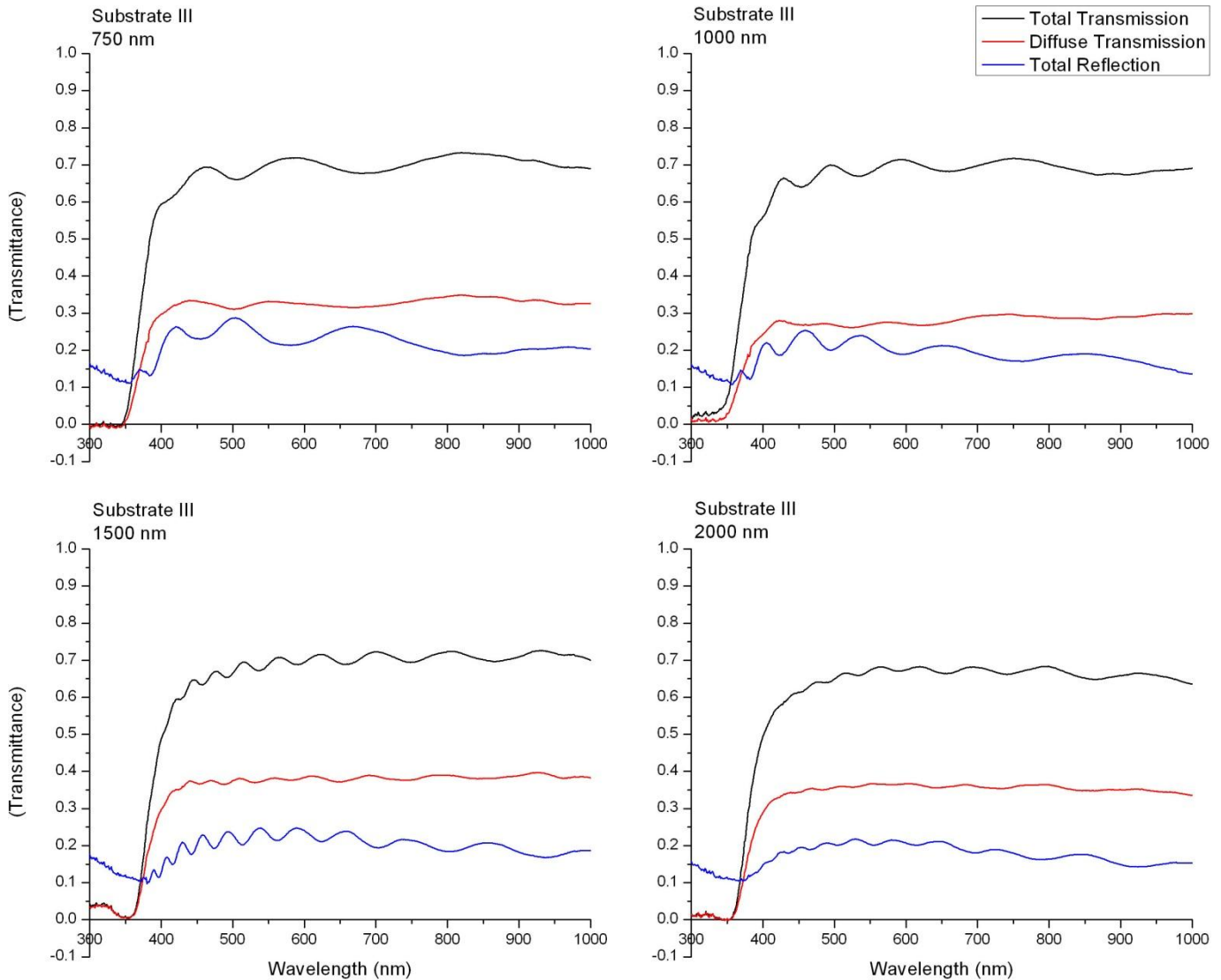


Figure 4.3 – Optical measurements results for Substrate III.

Here one can clearly see a difference between Substrate III and Substrates I and II. Substrate III has a micro-pyramidal structure with a base of around $10 \mu m$, compared to the other two which have a submicron-(anti)pyramidal structure with a base of around 400 nm . As we can see, the larger pyramids promote reflection, but also diffuse transmission. So less light is transmitted, but a larger

portion of the light that is transmitted is refracted. Either this reduces the efficiency because less light is being transmitted, or it increases efficiency because it increases the path of the light.

4.2 RESULTS OF SOLAR SIMULATOR MEASUREMENTS

As mentioned before, we unfortunately lost our 1500 nm substrates during the process of making solar cells out of them. Because we didn't have enough time to create another 1500 nm batch, we unfortunately only have data of our three other substrates. For the remaining solar cells, we did J-V measurements under the solar simulator. For every measurement, only a handful of the ± 30 cells in total were not shunted and had efficiencies of more than $\pm 2\%$. Each time I will show a pictograph illustrating the relative efficiencies of the cells. Grey cells are shunted cells (efficiency close to zero), and the blacker the cells are, the higher their efficiency.

Here I will summarize the results, but in the chapter "Tables and Figures", you can find for each substrate a picture of the J-V curve (current density given in mA/cm^2) for those cells with high enough efficiencies (higher than 2%). And you can also find a more detailed table of each substrate, in which several physical quantities can be easily read out.

4.2.1 SUBSTRATE I-750

Here we can see a depiction of the performance of cells on the I-750 substrate. The top left cell is called A1 and the bottom left A2, all the way to the top right cell A29 and the bottom right cell A30.



Here we can see that more than half of the cells are shunted, eleven have efficiencies higher than 2%. This substrate has the most "good" cells than any other substrate. For the J-V curve and a more detailed table with some of the physical quantities you can click on the link below or just go to the appropriate subsection in the chapter "Tables and Figures". There we can see that the most efficient cell on this substrate is cell A14 with a conversion efficiency of $\eta_{conv} = 6.4\%$, with *Fill Factor* = **0.65**, $J_{sc} = 11.5 mA/cm^2$ and $V_{oc} = 0.8609 V$.

Go to Graph & Table of Substrate I-750.

4.2.2 SUBSTRATE I-1000

For the I-1000 substrate, only six cells had efficiencies higher than 2%. As can be seen in the picture below.



The highest efficiency cell is A23 with $\eta_{conv} = 3.8\%$, $FF = 0.45$, $J_{sc} = 9.68 mA/cm^2$ and $V_{oc} = 0.8532 V$. All three numbers are less than that with the I-750 substrate.

Go to Graph & Table of Substrate I-1000.

4.2.3 SUBSTRATE I-2000

Our next substrate, I-2000, has seven non shunted cells.



The highest efficiency cell for this substrate is the A18 cell with an efficiency of $\eta_{conv} = 3.1\%$, with $FF = 0.43$, $J_{sc} = 11.5 \text{ mA/cm}^2$ and $V_{oc} = 0.8648 \text{ V}$. All three numbers are again less than that with the I-750 substrate and also slightly less than that with the I-1000 substrate.

Go to Graph & Table of Substrate I-2000.

4.2.4 SUBSTRATE II-750

Going to Substrate II, the II-750 substrate has seven good cells. The highest efficiency being the cell number A14 with $\eta_{conv} = 6.2\%$, $FF = 0.62$, $J_{sc} = 11.8 \text{ mA/cm}^2$ and $V_{oc} = 0.8497 \text{ V}$. These numbers are comparable with the I-750 Substrate. The efficiency here is somewhat less, but not significantly low.



Go to Graph & Table of Substrate II-750.

4.2.5 SUBSTRATE II-1000

For this Substrate, II-1000, there were ten good cells as can be seen below. The most efficient cell, A23, has an efficiency of $\eta_{conv} = 4.2\%$, with $FF = 0.48$, $J_{sc} = 9.86 \text{ mA/cm}^2$ and $V_{oc} = 0.8752 \text{ V}$.



Go to Graph & Table of Substrate II-1000.

4.2.6 SUBSTRATE II-2000

Only three cells were good with Substrate II-2000. The highest efficiency cell being A14 with $\eta_{conv} = 3.2\%$, $FF = 0.42$, $J_{sc} = 8.86 \text{ mA/cm}^2$ and $V_{oc} = 0.8581 \text{ V}$. Because there are only three good cells, this is not considered to be a very reliable measurement.



Go to Graph & Table of Substrate II-2000.

4.2.7 SUBSTRATE III-750

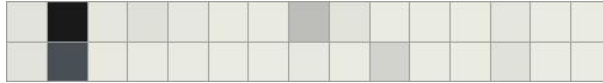
Again measurements with Substrate III-750 might not be very reliable because there are only four cells with high enough efficiencies. The highest being A05 with $\eta_{conv} = 5.4\%$, $FF = 0.62$, $J_{sc} = 10.3 \text{ mA/cm}^2$ and $V_{oc} = 0.8495 \text{ V}$.



Go to Graph & Table of Substrate III-750.

4.2.8 SUBSTRATE III-1000

Here we see only two good cells. This is not enough to get reliable results. Despite this we do measure a highest efficiency in cell A03 with $\eta_{conv} = 2.6\%$, $FF = 0.36$, $J_{sc} = 9.50 \text{ mA/cm}^2$ and $V_{oc} = 0.7781 \text{ V}$.



Go to Graph & Table of Substrate III-1000.

4.2.9 SUBSTRATE III-2000

With our last Substrate, III-2000, we get nine good cells. Although there are relatively a lot of good cells, the highest efficiency cell, A13, has an efficiency of only $\eta_{conv} = 3.7\%$, with $FF = 0.46$, $J_{sc} = 9.61 \text{ mA/cm}^2$ and $V_{oc} = 0.8314 \text{ V}$.



Go to Graph & Table of Substrate III-2000.

5 CONCLUSION

5.1 OPTICAL MEASUREMENTS CONCLUSION

From the optical measurements we can conclude that the two submicron-(anti)pyramidal substrates I and II behave more or less the same. Most of the light is transmitted, of which only a small fraction is scattered (diffuse transmission is between 0% and 5%). Also a small portion, between 10% and 20%, is reflected back.

When compared to the micro-pyramidal substrate III, we can see a big difference. Here a larger portion of the light is reflected back (between 15% and 30%), at the same time we also can see a larger portion of the transmitted light being refracted, between 30% and 35%. So even though less light is being transmitted, this does not necessarily mean that cells deposited on Substrate III will be less efficient. Because a larger portion of the light that does get transmitted is refracted, the transmitted light, therefore, covers a longer path through the active material. Measurements with the Solar Simulator will be able to tell us which substrate is the most efficient.

5.2 SOLAR SIMULATOR MEASUREMENTS CONCLUSION

If we compare the different thicknesses of aluminum doped zinc-oxide of each substrate in the optical measurements, we can see that there is no significant difference between them. The

transmission for lower wavelengths seems to even get slightly better with higher thickness. Also a slightly larger diffuse transmission can be seen for the 750 nm substrates I and II. This might mean that for larger TCO thickness, the surface of our substrate is flattened slightly, causing less light to be refracted by the pyramidal structures.

For the Solar Simulator measurements, we made a table below (see Table 5.1) with the efficiency, Fill Factor short circuit current density J_{sc} and open circuit voltage V_{oc} , of the best cell of each substrate. And as one can see, the Fill Factor is a fairly good indicator of this conversion efficiency. The higher the FF, the higher the efficiency. The V_{oc} is a measure for the amount of recombination in a cell. Therefore it gives information about the amount of defects at the surface caused by texturing. Furthermore the J_{sc} will give us an indication of the light trapping effectiveness as it is proportional to the irradiance through the substrate. Note that we have indicated substrates with less than four good cells with an asterisk, as their efficiencies might not be as accurate.

Substrate	Efficiency	Fill Factor	J_{sc} [mA/cm ²]	V_{oc} [V]
I-750	6.4%	0.65	11.5	0.8609
I-1000	3.8%	0.45	9.68	0.8532
I-2000	3.1%	0.43	8.46	0.8648
II-750	6.2%	0.62	11.8	0.8497
II-1000	4.2%	0.48	9.86	0.8752
II-2000 *	3.2%	0.42	8.86	0.8581
III-750	5.4%	0.62	10.3	0.8495
III-1000 *	2.6%	0.36	9.50	0.7781
III-2000	3.7%	0.46	9.61	0.8314

Table 5.1 - Maximum efficiency, Fill Factor and short circuit current density and open circuit voltage of best cells per substrate.

If we take a look at Table 5.1, we can see that, for each substrate, the efficiency decreases for greater TCO thicknesses. The highest efficiency, 6.4%, is measured for Substrate I-750. But this is not significantly higher than the 6.2% of Substrate II-750. Hence, as with the optical measurements, we can see no significant differences between the submicron-pyramidal and submicron-antipyramidal structured substrates.

Also, we can see that both Substrate I and II, for 750 nm TCO thickness, have significantly higher efficiencies than Substrate III-750. The efficiency for the 1000 nm Substrates I and II is also higher than Substrate III. But for the largest thickness, 2000 nm, Substrate III is the most efficient.

Furthermore, there is a decrease in current density J_{sc} for higher TCO thickness. Since J_{sc} is proportional to the irradiance through our substrate, we can conclude that the reason for the decreasing J_{sc} is either due to flattening of our substrate structures or less (total) transmission. Our

Perkin Elmer measurements, however, showed that there is no significant difference in the total transmissions of each substrate for our different TCO thicknesses (compare the four graphs in each figure of Figure 4.1, Figure 4.2 and Figure 4.3). Note that the decrease in J_{sc} is more significant for Substrates I and II than for Substrate III.

No significant difference or clear trend can be seen in the open circuit voltage numbers. Substrate III-1000 does show a significantly lower V_{oc} , but as stated before, the values for the substrates indicated with a star might not be very accurate.

From this we can conclude that the submicron-pyramidal substrates are more efficient than the micro-pyramidal substrates for smaller TCO thicknesses, but the efficiency of the former drops as the TCO gets thicker. This is probably due to the fact that the sub-micron-pyramidal structures are more susceptible to flattening of the surface for a given TCO thickness as they are smaller than the micro-pyramidal structures of Substrate III. Efficiency for Substrate III drops less for higher TCO thickness and is therefore the most efficient substrate for higher TCO thicknesses.

6 DISCUSSION

There are several reasons why the conclusion in the preceding section might not be accurate. First of all the substrates might have been out too long before depositing a-Si solar cells on them. They might have deteriorated somewhat during that time. Also the substrates might not have been completely clean, as there was quite some time between deposition and measuring, which may also have affected the measurements.

In addition, there were only a couple of working (not shunted) cells on each substrate and the differences in efficiency between these working cells was quite large. So it might only be by chance that the I-750 Substrate came out as the substrate with the highest efficiency. There aren't enough working cells on each substrate to come to an accurate conclusion.

One other thing that affected our research was the movement of the research group to Eindhoven. For this reason there was not enough time to create another batch of 1500 nm substrates that was destroyed during the a-Si solar cell deposition. We would have liked to have more TCO thicknesses to compare with each other. One improvement for future experiments therefore could be to try even more thicknesses of ZnO:Al.

6.1 FURTHER RESEARCH

Since unfortunately our topology measurements with the AFM failed, one could, for further research, try to find type of measurement to get proper topology measurements. Maybe an electron microscope can be used for this purpose.

Furthermore, one other thing that might be interesting for further research is to investigate if one can combine a ZnO:Al covered micro-pyramidal structured substrate with hydrochloric acid (HCl) texture etching to get an even better light scattering (For inspiration see [2]). By using different HCl concentrations and various etching times, one could try to find an HCl treatment that results in even better light trapping.

7 ACKNOWLEDGEMENTS

I would like to thank a few people for making this research possible and for their contributions and efforts. First of all, I would like to thank Dr. Jatin Rath for making this research available to me and allowing me to work with the Device Physics group.

Additionally, I would especially like to thank Minne de Jong for his supervision and help with my research throughout this year. He put a lot of time and effort in explaining the theory and helped me a lot with my measurements and thesis. I would also like to thank him for always being available and for his patience.

Lastly I would like to thank Bart Sasbrink for taking care of all the solar cell depositions, and the rest of the group for their helpfulness and for the friendly atmosphere.

8 BIBLIOGRAPHY

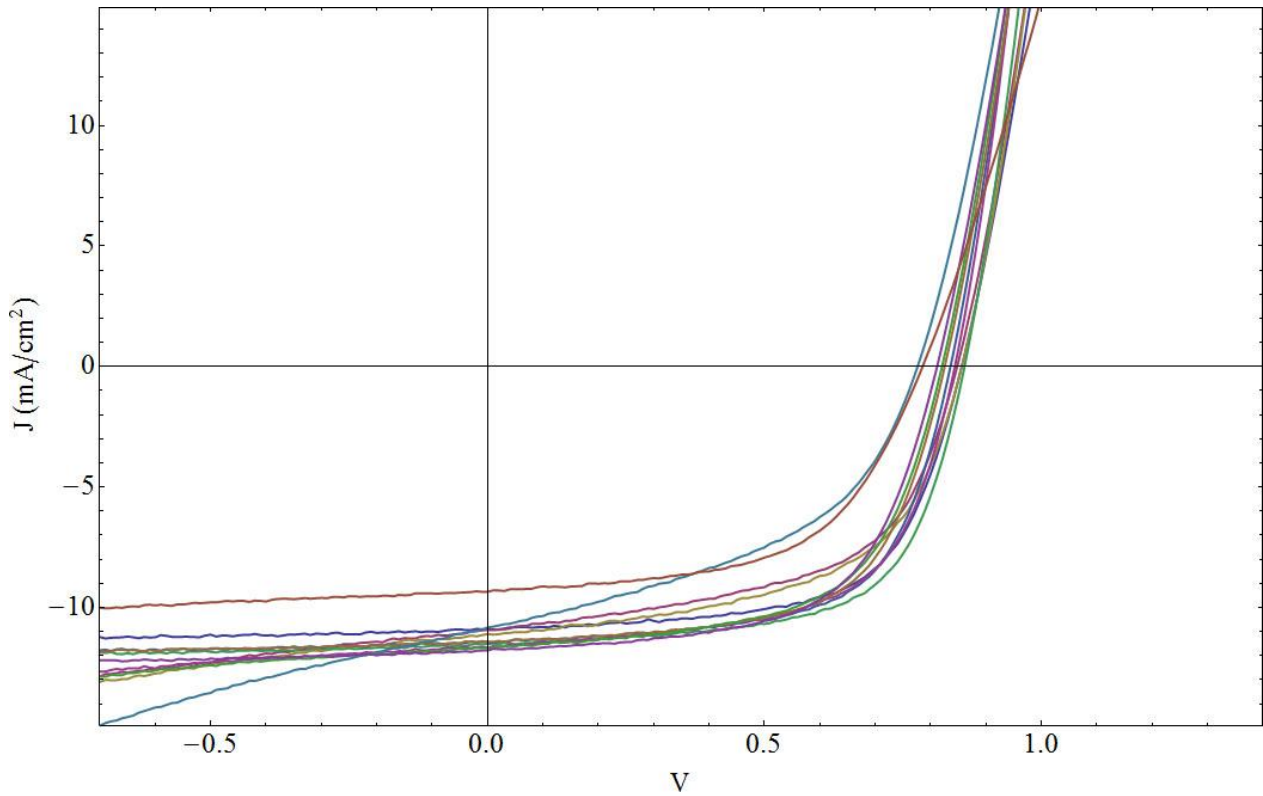
- [1] Jong, M.M. de; Rath, J.K.; Schropp, R.E.I.; Sonneveld, P.J.; Swinkels, G.L.A.M.; Holterman, H.J.; Baggerman, J.; Rijn, C.J.M. van, 2011. *Geometric Light Confinement in a-Si Thin Film Solar Cells On Micro-Structured Substrates*. Hamburg, Proceedings EUPVSEC 26, page number?.
- [2] Fernandez et al., 2011. *High Quality Textured ZnO:Al Surfaces Obtained By Two Step Wet-Chemical Etching Method For Application in Thin Film Silicon Solar Cells*, Solar Energy Materials & Solar Cells 95, 2281-2286
- [3] Häberlin, H., 2012. *Photovoltaics: System Design and Practice*. 1st ed. Chichester, West Sussex: Wiley.
- [4] Haug, F.-J., n.d. *Superstrate*. [Online]
Available at: <http://www.superstrate.net/pv/limit/index.html>
[Accessed 14 07 2012].
- [5] Hitoshi et al., 2011. *Flattened Light-Scattering Substrate in Thin Film Silicon Solar Cells For Improved Infrared Response*. sl, Appl. Phys. Lett. 98, 113502.
- [6] REN21 Steering Committee, 2012. *Renewables 2012: Global Status Report*, Paris: REN21 Secretariat.
- [7] Schropp, R. E. & Zeman, M., 1998. *Amorphous and Microcrystalline Silicon Solar Cells: Modeling, Materials and Device Technology*. 1st ed. Dordrecht, The Netherlands: Kluwer Academic Publishers.
- [8] Solomon, S. et al., 2007. *Climate Change 2007: The Physical Science Basis*, Cambridge: Cambridge University Press.
- [9] U.S. Energy Information Administration, 2011. *International Energy Outlook*, Washington: U.S. Energy Information Administration.
- [10] Wenham, S. R., Green, M. A., Watt, M. E. & Corkish, R., 2007. *Applied Photovoltaics*. 2nd ed. UK & USA: Earthscan.
- [11] Würfel, P., 2005. *Physics of Solar Cells: From Principles to New Concepts*. 1st red. Weinheim, Germany: Wiley-VCH.
- [12] Zeman, M., sd *Solar Cells*. Delft: Delft University of Technology.

9 TABLES AND FIGURES

9.1 SOLAR SIMULATOR TABLES AND FIGURES

Below you can find all tables and graphs of each substrate-thickness pair.

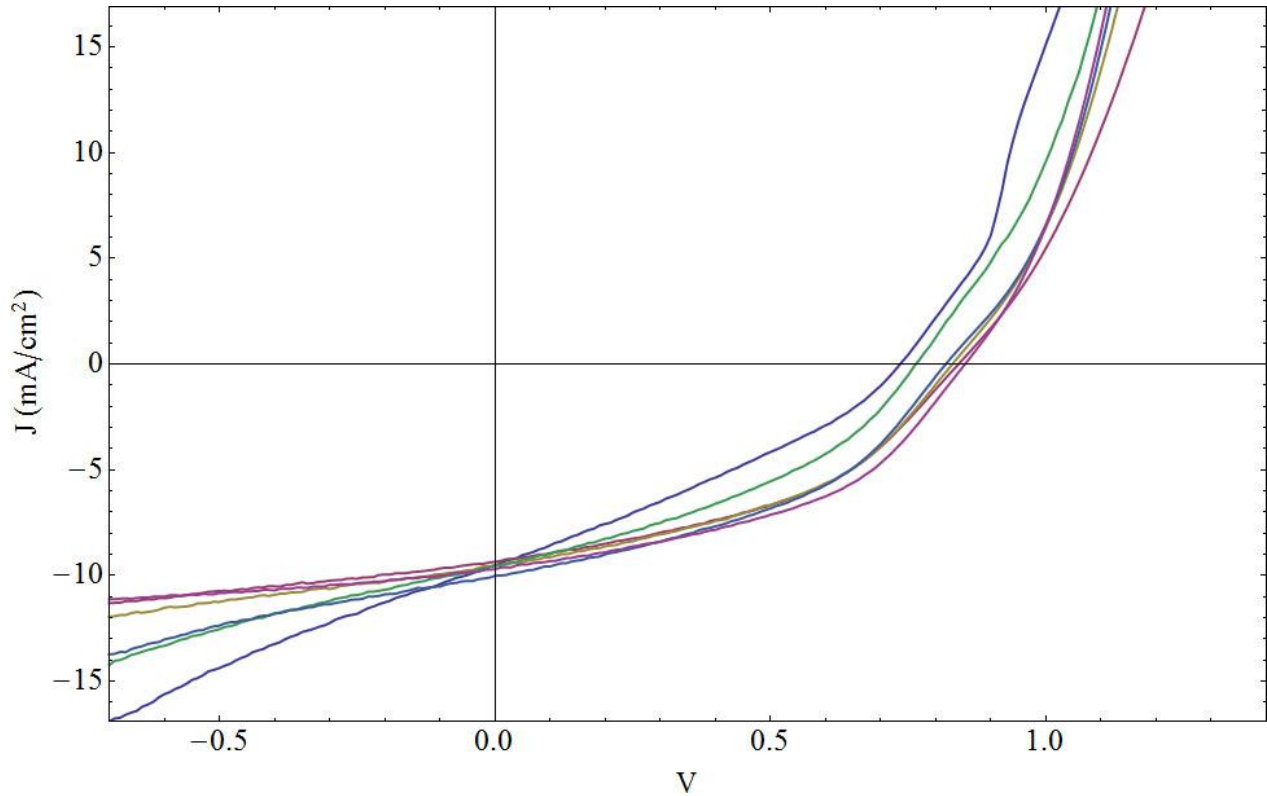
9.1.1 GRAPH & TABLE OF SUBSTRATE I-750



Cell #	N_{effcr} [%]	J_{sc} [mA/cm^2]	V_{oc} [V]	FF	R_s [Ωcm^2]	R_p [Ωcm^2]
A14	6.409	11.52	0.8609	0.6462	8.919	1206
A17	6.107	11.45	0.8357	0.6381	9.027	933.9
A18	6.046	11.65	0.8435	0.6154	9.334	896.2
A05	5.964	10.92	0.8560	0.6383	10.40	1144
A21	5.924	11.42	0.8253	0.6283	9.788	900.8
A24	5.810	11.77	0.8114	0.6084	10.72	889.4
A22	5.781	11.67	0.8204	0.6037	10.23	756.7
A08	5.320	11.13	0.8560	0.5584	10.52	474.1
A07	5.199	10.94	0.8477	0.5604	10.99	355.1
A27	4.145	9.332	0.7854	0.5654	17.34	774.0
A23	3.826	10.85	0.7763	0.4544	8.919	1206

Back to 4.2.1.

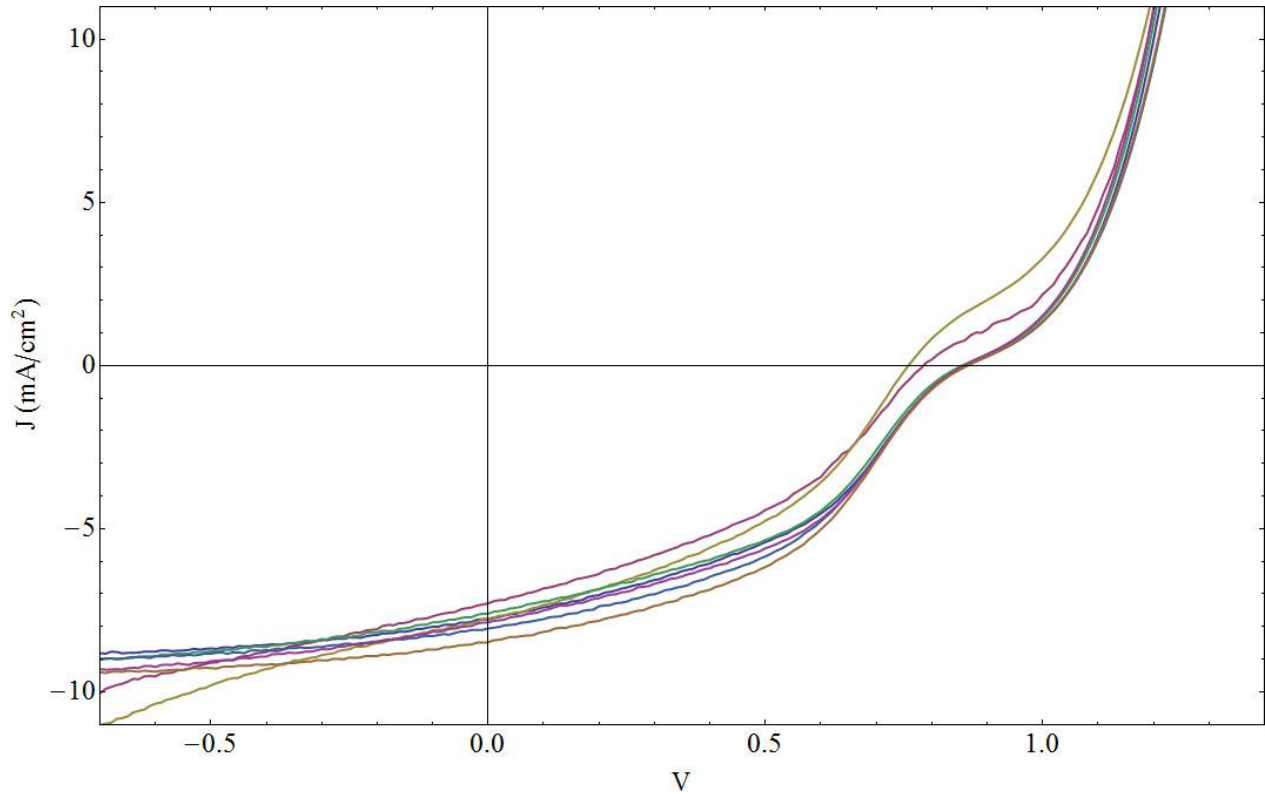
9.1.2 GRAPH & TABLE OF SUBSTRATE I-1000



Cell #	N_{effcr} [%]	J_{sc} [mA/cm^2]	V_{oc} [V]	FF	R_s [Ωcm^2]	R_p [Ωcm^2]
A23	3.756	9.683	0.8532	0.4546	30.21	290.8
A18	3.491	10.04	0.8184	0.4251	32.28	222.4
A02	3.441	9.347	0.8415	0.4375	35.03	266.9
A04	3.419	9.529	0.8303	0.4322	31.92	250.7
A06	2.773	9.536	0.7644	0.3805	28.02	172.3
A01	2.158	9.519	0.7356	0.3082	32.55	110.2

Back to Substrate I-1000.

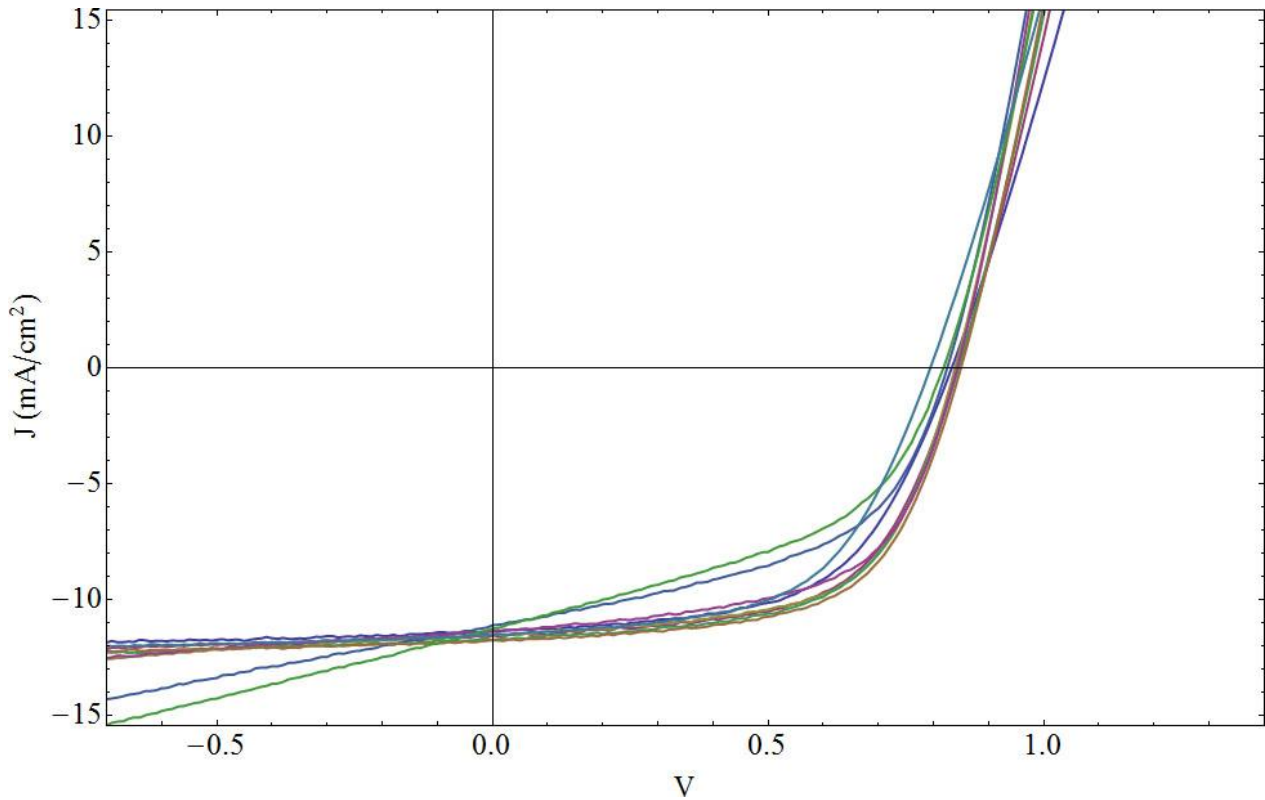
9.1.3 GRAPH & TABLE OF SUBSTRATE I-2000



Cell #	N_{effCr} [%]	J_{sc} [mA/cm^2]	V_{oc} [V]	FF	R_s [Ωcm^2]	R_p [Ωcm^2]
A18	3.131	8.463	0.8648	0.4278	113.6	393.3
A16	2.973	8.063	0.8628	0.4274	116.3	394.9
A17	2.885	7.855	0.8586	0.4277	112.0	302.7
A07	2.776	7.764	0.8631	0.4143	118.0	345.7
A15	2.740	7.583	0.8549	0.4226	114.9	301.0
A14	2.391	7.746	0.7583	0.4071	45.58	261.4
A13	2.226	7.277	0.7858	0.3893	72.73	240.6

Back to Substrate I-2000.

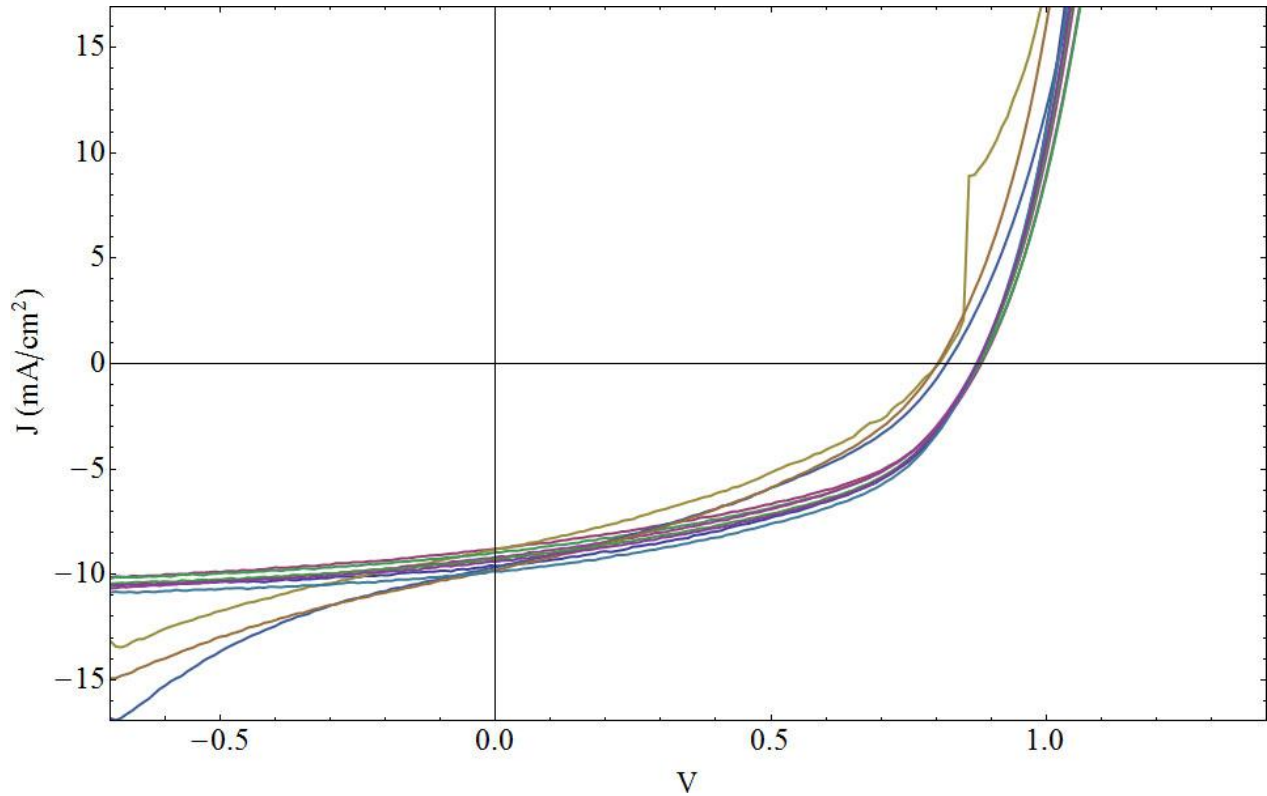
9.1.4 GRAPH & TABLE OF SUBSTRATE II-750



Cell #	N_{effcr} [%]	J_{sc} [mA/cm^2]	V_{oc} [V]	FF	R_s [Ωcm^2]	R_p [Ωcm^2]
A14	6.154	11.78	0.8497	0.6151	11.77	989.1
A10	5.983	11.74	0.8454	0.6030	12.28	937.9
A09	5.951	11.52	0.8392	0.6158	11.32	984.6
A08	5.891	11.60	0.8449	0.6010	13.35	853.1
A13	5.671	11.38	0.8429	0.5912	11.17	691.5
A04	5.485	11.37	0.8331	0.5789	15.82	838.9
A24	5.250	11.52	0.7942	0.5736	15.19	733.3
A11	4.593	11.15	0.8249	0.4996	13.31	219.8
A16	4.169	11.29	0.8178	0.4517	15.27	159.4

Back to Substrate II-750.

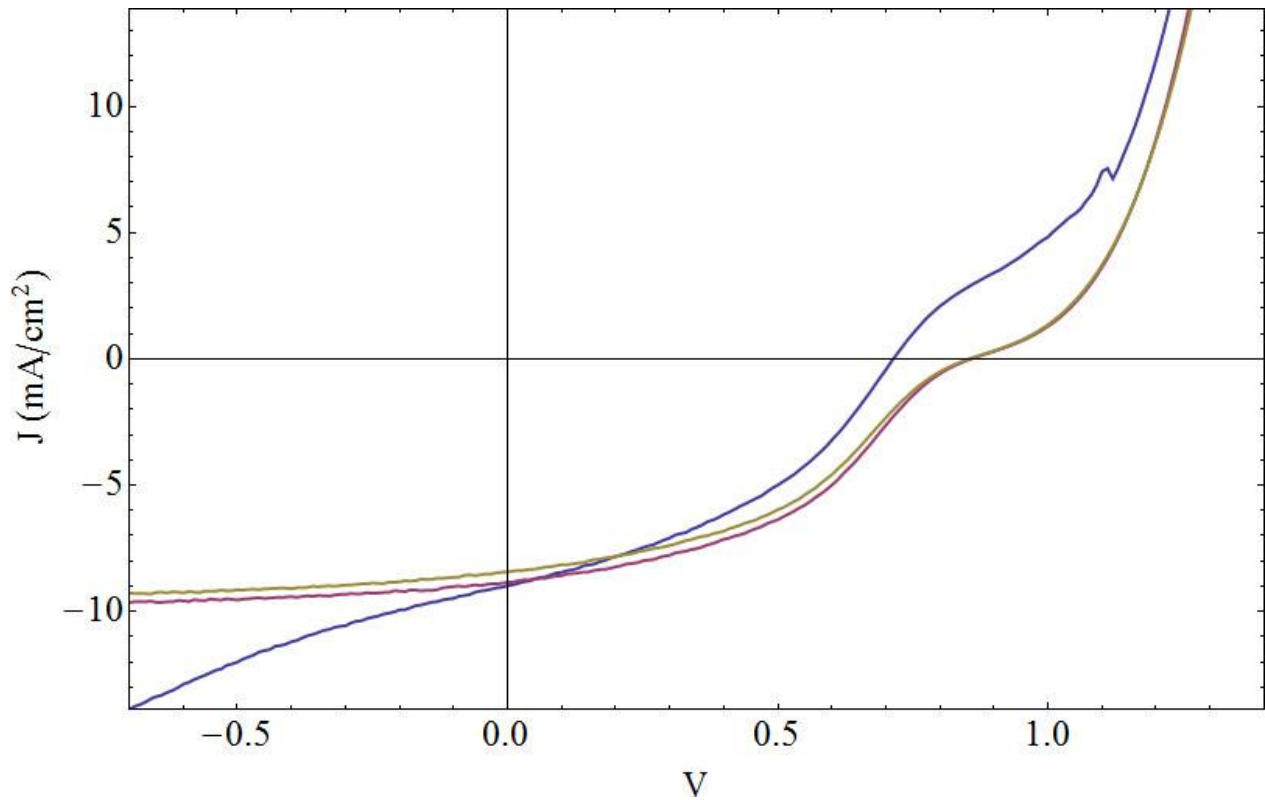
9.1.5 GRAPH & TABLE OF SUBSTRATE II-1000



Cell #	N_{effcr} [%]	J_{sc} [mA/cm^2]	V_{oc} [V]	FF	R_s [Ωcm^2]	R_p [Ωcm^2]
A23	4.164	9.858	0.8752	0.4827	17.35	361.5
A05	3.983	9.591	0.8770	0.4735	18.09	380.7
A24	3.951	9.383	0.8737	0.4820	19.22	357.2
A22	3.899	9.290	0.8759	0.4791	18.72	340.6
A20	3.731	9.182	0.8740	0.4649	20.50	330.8
A16	3.730	8.969	0.8790	0.4731	20.76	345.8
A12	3.638	8.785	0.8820	0.4696	20.53	325.0
A19	2.971	9.657	0.8191	0.3755	24.63	180.4
A21	2.952	9.794	0.8028	0.3755	24.00	179.1
A14	2.603	8.817	0.8049	0.3668	32.10	198.0

Back to Substrate II-1000.

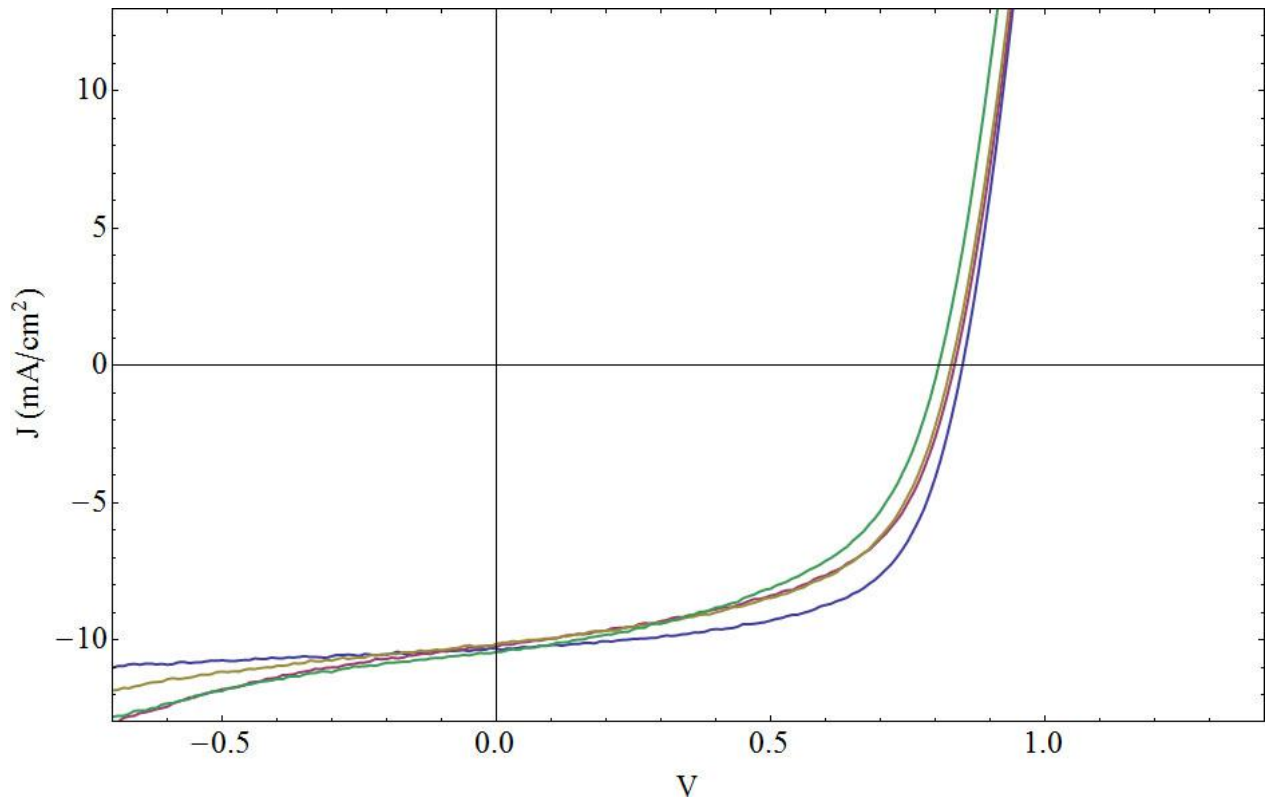
9.1.6 GRAPH & TABLE OF SUBSTRATE II-2000



Cell #	N_{effcr} [%]	J_{sc} [mA/cm^2]	V_{oc} [V]	FF	R_s [Ωcm^2]	R_p [Ωcm^2]
A14	3.198	8.856	0.8581	0.4208	129.8	429.2
A22	3.003	8.429	0.8545	0.4169	129.6	443.9
A12	2.549	8.990	0.7140	0.3970	32.85	207.3

Back to Substrate II-2000.

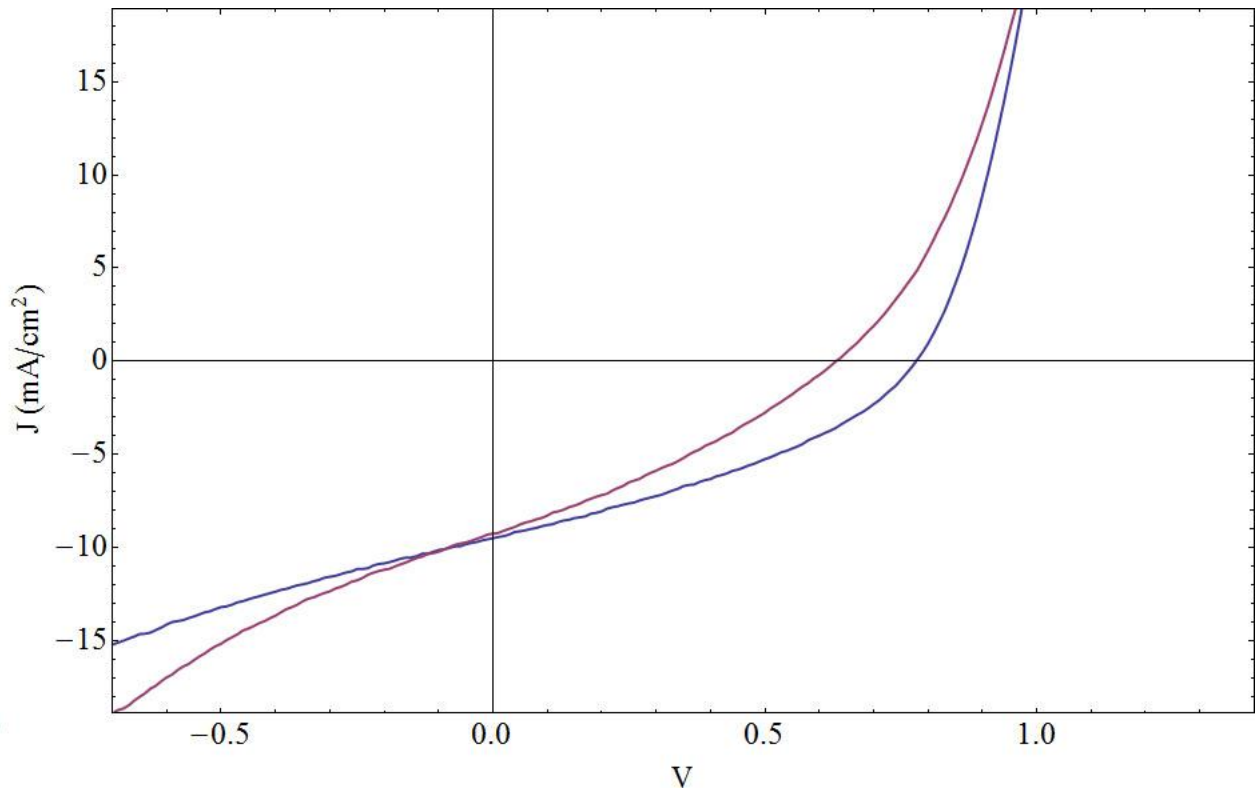
9.1.7 GRAPH & TABLE OF SUBSTRATE III-750



Cell #	N_{effcr} [%]	J_{sc} [mA/cm^2]	V_{oc} [V]	FF	R_s [Ωcm^2]	R_p [Ωcm^2]
A05	5.426	10.31	0.8495	0.6194	9.692	966.1
A08	4.671	10.14	0.8289	0.5557	11.55	489.9
A07	4.633	10.20	0.8351	0.5442	10.96	447.8
A13	4.276	10.44	0.8063	0.5081	11.89	435.1
A05	5.426	10.31	0.8495	0.6194	9.692	966.1

Back to Substrate III-750.

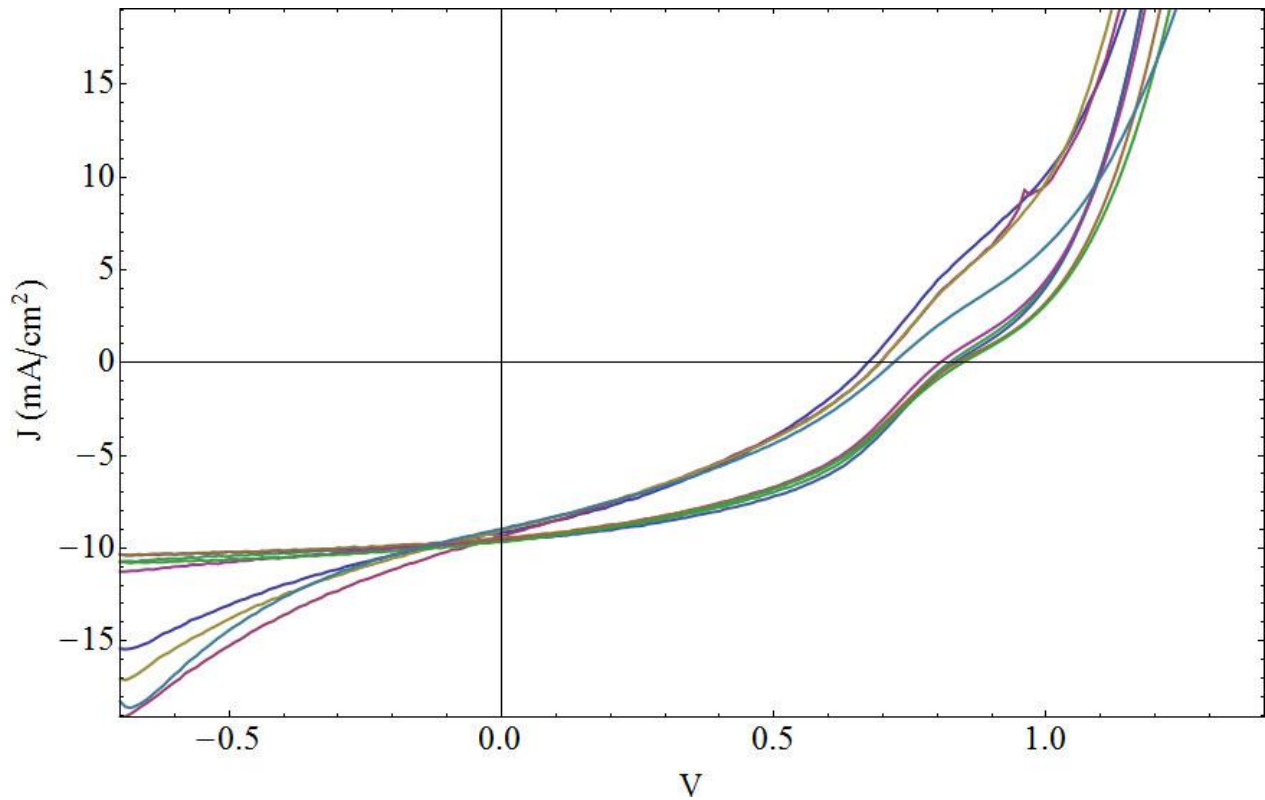
9.1.8 GRAPH & TABLE OF SUBSTRATE III-1000



Cell #	N_{effCr} [%]	J_{sc} [mA/cm^2]	V_{oc} [V]	FF	R_s [Ωcm^2]	R_p [Ωcm^2]
A03	2.644	9.505	0.7781	0.3575	24.81	144.6
A04	1.825	9.268	0.6313	0.3119	41.94	107.1

Back to Substrate III-1000

9.1.9 GRAPH & TABLE OF SUBSTRATE III-2000



Cell #	N_{effcr} [%]	J_{sc} [mA/cm^2]	V_{oc} [V]	FF	R_s [Ωcm^2]	R_p [Ωcm^2]
A13	3.689	9.610	0.8314	0.4617	48.69	435.8
A11	3.552	9.556	0.8222	0.4521	45.45	391.6
A26	3.441	9.658	0.8465	0.4209	57.51	324.2
A17	3.423	9.445	0.8361	0.4335	60.70	374.5
A15	3.380	9.529	0.8051	0.4406	44.33	335.5
A27	2.260	8.963	0.7195	0.3505	38.46	151.5
A03	2.211	9.168	0.6724	0.3587	31.90	175.0
A10	2.172	9.054	0.6935	0.3460	33.40	135.1
A09	2.151	9.330	0.6946	0.3318	33.76	119.5

Back to Substrate III-2000.